

Markov Subsampling based on Huber Criterion

Tieliang Gong, Yuxin Dong, Hong Chen, Bo Dong, Chen Li

Abstract—Subsampling is an important technique to tackle the computational challenges brought by big data. Many subsampling procedures fall within the framework of importance sampling, which assigns high sampling probabilities to the samples appearing to have big impacts. When the noise level is high, those sampling procedures tend to pick many outliers and thus often do not perform satisfactorily in practice. To tackle this issue, we design a new Markov subsampling strategy based on Huber criterion (HMS) to construct an informative subset from the noisy full data; the constructed subset then serves as a refined working data for efficient processing. HMS is built upon a Metropolis-Hasting procedure, where the inclusion probability of each sampling unit is determined using the Huber criterion to prevent over scoring the outliers. Under mild conditions, we show that the estimator based on the subsamples selected by HMS is statistically consistent with a sub-Gaussian deviation bound. The promising performance of HMS is demonstrated by extensive studies on large scale simulations and real data examples.

Index Terms—Markov chain, subsampling, robust inference, regression.

I. INTRODUCTION

RAPID advancement in modern science and technology introduces data with extraordinary size and complexity, which brings great challenges to conventional machine learning and statistical methods. In the literature, two fundamental approaches have emerged to tackle the challenges of big data: one is the divide-and-conquer strategy [1], which involves partitioning the data into manageable segments, implementing a particular algorithm on these data segments in parallel, and synthesizing a global output by aggregating the segmental outputs; the other approach is the subsampling strategy [2], which involves selecting a representative subset from the full data as a surrogate, and obtaining an output through further analyzation of the surrogate. The divide-and-conquer strategy usually relies on high computational power with computing clusters and is particularly effective when a dataset is too big to fit in one computer. However, it still consumes considerable computational resources and the access of distributed computational platforms are restricted by high cost. As a computationally cheaper alternative, subsampling gains its merit for the situation, when the computational resources are limited.

The key task of subsampling is to effectively identify important samples in order to maintain the essential information of the full data. This task is particularly challenging for big data, which often comes with poor quality (high noise level) due to the uncontrolled collecting process. In the literature,

informative sampling strategies are commonly adopted, where important samples are given high probabilities to be selected. During the last two decades, extensive studies have been concluded on informative sampling e.g. statistical leverage score method [3], [4], [5], [6], gradient method [7] and influence function method [8] etc. Leverage score subsampling assigns the sampling probabilities proportional to a distance measure within the covariates. It does not take into account the response and hence is sensitive to outliers. Both gradient-based subsampling and influence function based subsampling are using the response together with the covariates to design sampling patterns, in which the probabilities are computed proportional to the quadratic loss gradient or influence function. Although they do avoid the interference of outliers to some extent, the estimators calculated upon the associated subsamples are highly dependent on a reliable pilot model, which may be difficult to obtain in highly noisy setup.

Huber criterion [9] provides an effective way to deal with this situation. It is a hybrid of square loss for relatively small errors and absolute loss for relative large ones and hence is robust to heavy-tailed errors and outliers. Recent studies have shown the great potential of Huber criterion for robust estimation and inference. For example, [10] proposed to combine the Huber criterion and adaptive penalty as lasso and shows that the resulting estimator is more robust than adaptive LASSO in prediction and variable selection tasks. [11] developed data-driven Huber-type methods for regression tasks and establishes sub-Gaussian type concentration bounds for the Huber-type estimator. In [12], the adaptive Huber regression method was proposed, which significantly outperforms least squares both in terms of mean and standard deviation. Besides, it admits exponential type concentration bounds when the error variables have finite moments. [13] investigated the non-asymptotic consistency of ℓ_1 regularized robust M-estimator with Huber loss under Markov chain setting. [14] additionally investigated collinearity and explored the grouping effect in Huber regression. [15] proposed an alternative probabilistic interpretation of minimizing the Huber loss, which is equivalent to minimizing an upper-bound on the Kullback-Leibler (KL) divergence in Laplacian settings. [16] achieved robust forecasting based on Huber criterion for both non-Gaussian and non-stationary data.

In light of these advances, we aim to design a robust subsampling procedure by adopting the Huber criterion. To this end, this paper proposes a Markov subsampling strategy based on Huber criterion (HMS) for linear regression. The procedure is as follows: we first obtain a rough estimator β_0 based on a simple pilot selection, which determines the importance of each sample by calculating the Huber loss; we then perform subsampling from the full data \mathcal{D} to generate a subset \mathcal{D}_S through Metropolis-hasting (MH) type procedure, where the sampling probability is assigned according to the

T. Gong, Y. Dong, C. Li are with the School of Computer Science and Technology, Xi'an Jiaotong University, Xi'an, Shaanxi 710049, China, (e-mail: adidasgtl@gmail.com; dongyuxin@stu.xjtu.edu.cn; cli@xjtu.edu.cn).

B. Dong is with the School of Continuing Education, Xi'an Jiaotong University, Xi'an, 710049, e-mail: dong.bo@mail.xjtu.edu.cn.

H. Chen is with the College of Science, Huazhong Agriculture University, Wuhan, 430070, email: chenlh@mail.hzau.edu.cn.

Huber loss. By doing so, samples with large Huber loss are unlikely to be selected and hence the noisy samples and outliers are ruled out with high probability. Moreover, MH sampling procedure and its variants require a proposal distribution to specify the sample importance, which is crucial to the success (e.g. fast convergence rate) of these algorithms, as improper selection of proposal distribution may result in misleading estimates. Different from MH-type algorithms, HMS determines the sample importance directly by Huber criterion, where the turning parameter is pre-specified through data-driven strategy, hence avoids such a problem.

Our contributions are summarized as follows:

- We develop a distribution-free Markov subsampling strategy based on Huber criterion to construct an informative subset from the noisy full data, which further enables robust statistical inference and prediction.
- Theoretically, we establish the statistical consistency for the regression estimator based on the subsample suggested by HMS in terms of Bahadur type representation [17], [18]. Our results indicate that, with an appropriate robust parameter, the HMS-based estimator achieves nearly optimal convergence rate. The theoretical results also extends the error analysis of Huber estimator under i.i.d. samples to Markov dependent setup.
- Extensive empirical studies verify our theoretical findings. The promising performance of HMS estimator is also supported by both large-scale simulations and real data examples.

The rest of the paper is organized as follows. Sections II sets the notations and problem statement. Section III introduces the proposed Markov subsampling algorithm based on the Huber criterion. Section IV establishes the asymptotic analysis and the corresponding error bounds of the subsampling estimator. Section V demonstrates experimental results on both simulation studies and real data examples. Section VI concludes our work.

II. NOTATIONS AND PRELIMINARIES

A. Notations

To make our arguments in the following section precise, some concepts and notations being used throughout this paper are introduced.

Let $\mathbf{u} = (u_1, u_2, \dots, u_d)^\top \in \mathbb{R}^d$ and $p \geq 1$, we denote the ℓ_p -norm and ℓ_∞ -norm of \mathbf{u} as $\|\mathbf{u}\|_p = (\sum_{i=1}^d |u_i|^p)^{1/p}$, $\|\mathbf{u}\|_\infty = \max_{j \in [1, d]} |u_j|$. For any $\mathbf{w} \in \mathbb{R}^d$, $\langle \mathbf{u}, \mathbf{w} \rangle = \mathbf{u}^\top \mathbf{w}$. For two scalars a, b , let $a \wedge b = \min\{a, b\}$ and $a \vee b = \max\{a, b\}$. Given a matrix $\mathbf{A} \in \mathbb{R}^{m \times n}$, the corresponding spectral norm is defined by $\|\mathbf{A}\| = \max_{\mathbf{u} \in \mathbb{S}^{n-1}} \|\mathbf{A}\mathbf{u}\|_2$, where \mathbb{S}^{n-1} is the unit sphere in \mathbb{R}^n . If $\mathbf{A} \in \mathbb{R}^{n \times n}$, we denote the minimum and maximum eigenvalue of \mathbf{A} by $\lambda_{\min}(\mathbf{A})$ and $\lambda_{\max}(\mathbf{A})$. For a function $f : \mathbb{R}^d \rightarrow \mathbb{R}$, we denote its gradient vector by $\nabla f \in \mathbb{R}^d$.

Definition 1: [19] A random variable $X \in \mathbb{R}$ is said to be sub-Gaussian with variance proxy σ^2 if $\mathbb{E}[X] = 0$ and its moment generating function satisfies

$$\mathbb{E}[\exp(sX)] \leq \exp\left(\frac{s^2\sigma^2}{2}\right), \quad \forall s \in \mathbb{R}. \quad (1)$$

The following concepts are important in our theoretical analysis. Let $\{X_i\}_{i \geq 1}$ be a Markov chain on a general space \mathcal{X} with invariant probability distribution π . Let $P(x, dy)$ be a Markov transition kernel on a general space $(\mathcal{X}, \mathcal{B}(\mathcal{X}))$ and P^* be its adjoint. Denote $\mathcal{L}_2(\pi)$ by the Hilbert space consisting of square integrable functions with respect to π . For any function $h : \mathcal{X} \rightarrow \mathbb{R}$, we write $\pi(h) := \int h(x)\pi(dx)$. Define the norm of $h \in \mathcal{L}_2(\pi)$ as $\|h\|_\pi = \sqrt{\langle h, h \rangle}$. Let $P^t(x, dy)$, ($t \in \mathbb{N}$) be the t -step Markov transition kernel corresponding to P , then for $i \in \mathbb{N}$, $x \in \mathcal{X}$ and a measurable set S , $P^t(x, S) = \Pr(X_{t+i} \in S | X_i = x)$. Following the above notations, we introduce the definitions of ergodicity and spectral gap for a Markov chain.

Definition 2: Let $M(x)$ be a non-negative function. For an initial probability measure $\rho(\cdot)$ on $\mathcal{B}(\mathcal{X})$, a Markov chain is uniformly ergodic if

$$\|P^t(\rho, \cdot) - \pi(\cdot)\|_{TV} \leq T(x)t^n \quad (2)$$

for some $T(x) < \infty$ and $t < 1$, where $\|\cdot\|_{TV}$ denotes total variation norm.

A Markov chain is geometrically ergodic if (2) holds for some $t < 1$, which eliminates the bounded assumption on $T(x)$. The dependence of a Markov chain can be characterized by the absolute spectral gap, defined as follows.

Definition 3: (Absolute spectral gap) A Markov operator P has a \mathcal{L}_2 spectral gap $1 - \lambda$ if

$$\lambda(P) := \sup \{\|Ph\|_\pi : \|h\|_\pi = 1, \pi(h) = 0\} < 1. \quad (3)$$

The quantity $1 - \lambda$ measures the convergence speed of a Markov chain towards its stationary distribution π [20]. A smaller λ usually implies faster convergence speed and less variable dependence.

B. Huber Regression

In this paper, we consider the data generated from the following linear regression model

$$y_i = \langle \mathbf{x}_i, \boldsymbol{\beta}^* \rangle + \varepsilon_i, \quad i = 1, 2, \dots, n \quad (4)$$

where y_i is the response, $\mathbf{x}_i \in \mathbb{R}^d$ is the covariate, ε_i is the error and $\boldsymbol{\beta}^* \in \mathbb{R}^d$ is the regression coefficient. It is well known that the ordinary least square estimator $\boldsymbol{\beta}_{ols}$ for (4) has a suboptimal polynomial-type deviation bound, which makes it inappropriate for large scale estimation and inference. The key factor lies in the sensitivity of square loss to outliers [21]. To overcome this drawback, Huber loss [9], [12] is proposed for achieving robust estimation. The Huber loss is defined by

$$\ell_\tau(x) = \begin{cases} x^2/2, & \text{if } |x| \leq \tau, \\ \tau|x| - \tau^2/2, & \text{if } |x| > \tau, \end{cases} \quad (5)$$

where $\tau > 0$ is the robustification parameter that controls the bias and robustness. This function is quadratic with small values of τ while grows linearly for large values of τ . The specification of τ is critical in practical applications. Some recent studies on deviation bounds of Huber regression [12], [11] suggest that τ should be adaptive with the dimension of input space, the moment condition of the noise distribution and the sample size to achieve robustness and unbiasedness estimate.

Specifically, Sun et al. [12] obtained near-optimal deviation bounds of Huber regression for both low and high dimensional cases. These observations will motivate us to derive optimal bounds for HMS estimation.

Define the empirical loss function $L_\tau(\beta) = \frac{1}{n} \sum_{i=1}^n \ell_\tau(y_i - \langle \mathbf{x}_i, \beta \rangle)$. The object of Huber regression is to find an optimizer of the following convex optimization problem

$$\beta_\tau^* = \arg \min_{\beta \in \mathbb{R}^d} L_\tau(\beta), \quad (6)$$

which can be easily solved via the iteratively reweighted least square method [22]. Denote the derivative of Huber loss $\ell_\tau(x)$ as φ_τ , i.e

$$\varphi_\tau = \text{sign}(x) \min\{|x|, \tau\}, \quad x \in \mathbb{R}. \quad (7)$$

In this paper, we focus on the setting that $n \gg d$. Denote \mathbf{X}_S by the subsample matrix produced by HMS and $\bar{\mathbf{x}} = \Sigma^{-1/2} \mathbf{x}$. Suppose that $\Sigma = \mathbb{E}_\pi(\mathbf{X}_S \mathbf{X}_S^\top)$ is positive definite, the regression errors ε_i satisfy $\mathbb{E}(\varepsilon_i | \mathbf{x}_i) = 0$ and $v_{i,\delta} = \mathbb{E}(|\varepsilon_i|^{1+\delta} | \mathbf{x}_i) < \infty$. With this setup, we write

$$v_\delta = \frac{1}{n} \sum_{i=1}^n v_{i,\delta} \quad \text{and} \quad u_\delta = \min\{v_\delta^{1/(1+\delta)}, \sqrt{v_1}\}, \quad \delta > 0.$$

III. MARKOV SUBSAMPLING BASED ON HUBER CRITERION

As discussed before, the currently used informative measures (leverage score, gradient, influence function) in subsampling may not reflect the real contribution of each sample in highly-noisy settings, hence the resulting estimator can be misleading. To alleviate this issue, we develop a Markov subsampling strategy based on Huber criterion (HMS) to achieve robust estimation. The core idea is to select the samples with small errors based on Huber criterion by Markov chain Monte Carlo (MCMC) method. Concretely, HMS consists of three steps: 1) pilot estimation; 2) Huber loss calculation; 3) Markov subsampling.

- **Pilot estimation.** The idea of pilot is widely applied in subsampling procedure [7], [8], [23], [24], where the sampling probability is specified by a pilot estimation. A popular way for calculating pilot is uniform subsampling. To avoid bringing additional computational burden, we suggest the pilot β_0 to be calculated by least square criterion based on a small random subset with user preference size $d < r \ll n$, i.e. $\beta_0 = (\mathbf{X}_r^\top \mathbf{X}_r)^{-1} \mathbf{X}_r^\top \mathbf{y}_r$. It only takes additional $\mathcal{O}(rd^2)$ CPU time. We empirically demonstrate that HMS estimator does not rely heavily on the quality of β_0 .
- **Huber loss calculation.** The robustification parameter τ in Huber criterion plays a trade-off role between the bias and robustness. In practical, τ is usually set to be fixed through 95% asymptotic efficiency rule [9], [18], [25], [26]. However, a fixed value may not guarantee a good estimator, especially in highly noisy cases. As illustrated in Figure 1, τ should be adapted with n, d (consider that $n \gg d$, we ignore the effect of d). It can be seen that there exists some τ such that the AME of β_0 achieves minimum for a fixed sample size n . In practical, we first restrict τ in a reasonable range and select the optimal value then

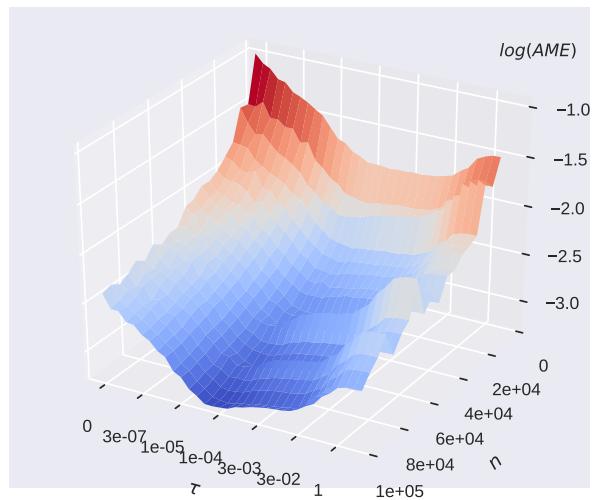


Fig. 1: $\log(\text{AME})$ versus τ and n (AME: Averaged Mean Error, defined in 43). Here, we generate the data by (4) with $n = 1M$, $d = 500$ and ε_i are i.i.d from student-t distribution with degree of freedoms 2.

according to the minimal AME principal. After specifying τ , the importance of a sample (\mathbf{x}_i, y_i) can be measured by the corresponding Huber loss $\ell_\tau(y_i - \mathbf{x}_i^\top \beta_0)$. The greater importance of a sample often comes with smaller Huber loss.

- **Markov subsampling.** It has been shown that the Markov chain samples may lead to more robust estimation than i.i.d counterparts in machine learning [27] and optimization tasks [28], [29]. With this in mind we tend to implement probabilistic sampling through a Metropolis-Hasting type procedure. The core step, probabilistic acceptance rule, is designed based on Huber criterion. Concretely, at some current sample \mathbf{z}_t , a randomly selected candidate sample \mathbf{z}^* is accepted with probability defined in (8). If \mathbf{z}^* is accepted, we set $\mathcal{D}_S = \mathcal{D}_S \cup \mathbf{z}^*$ and $\mathbf{z}^* = \mathbf{z}_{t+1}$. Otherwise, we randomly select a sample as a candidate and repeat this process. Finally, we accept the last n_{sub} elements generated by this procedure after a user-specified burn-in period.

The detailed procedures are summarized in Algorithm 1. Note that the probabilistic acceptance rule (8) tends to select the samples with small Huber loss with high probability. Moreover, the subsamples generated by Algorithm 1 constitute an irreducible Markov chain, and therefore are uniformly ergodic [30], [31]. Computationally, HMS takes $\mathcal{O}(n_0 d^2)$ time for pilot estimation, $\mathcal{O}((n_{sub} + t_0)d)$ time for Metropolis-Hasting sampling procedure and $\mathcal{O}(n_{sub} d^2)$ time for optimizing (6) (L-BFGS-B optimization strategy [32] is adopted). Hence, the total time complexity is $\mathcal{O}((2n_{sub} + t_0)d^2)$, which is much saving computational cost since $n_{sub}, t_0 \ll n$.

IV. THEORETICAL ASSESSMENTS OF HMS ESTIMATOR

In this section, we provide theoretical support for the proposed HMS. In particular, we aim at bounding the difference between the HMS estimator β_τ and the oracle β^* . Previous

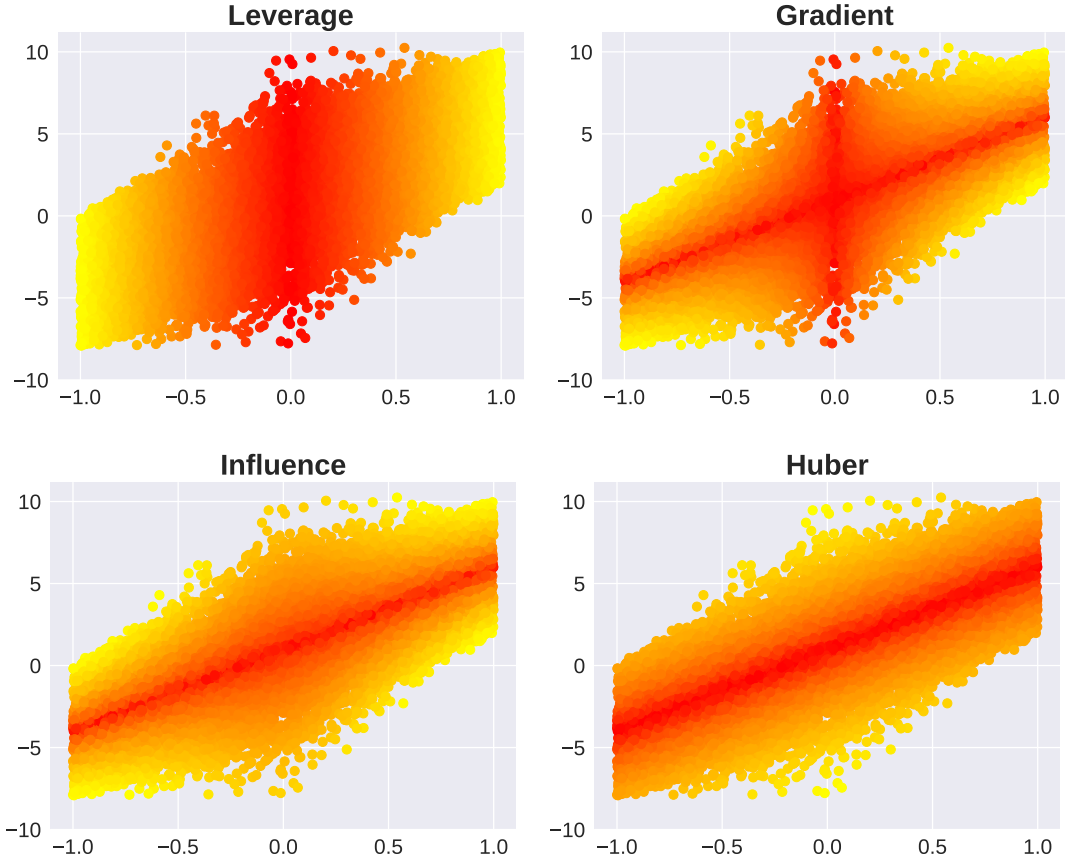


Fig. 2: Illustration of sampling probabilities with different importance measures. The data are generated by $y = 5x + 1 + \varepsilon$ with $n = 10000$ and ε is a mixture of Gaussian and uniform distribution. The bright yellow and red represent high and low sampling probability respectively. Both leverage score and gradient are incline to select the points with large residuals near the center. The Influence tends to balance the regression design and the residual. The HMS can further enhance the effect of the influence.

theoretical studies on subsample estimator are based on least squares [2], [5], [7], which has a closed-form solution. However, HMS estimator does not admit an explicit close-form representation and the robustification parameter τ is not fixed, all these pose the difficulties for analyzing its statistical properties. To overcome these issues, we adopt the Lepski-type method developed in [12]. We first present several necessary assumptions as below.

Assumption 1: [30] (Non-zero spectral gap Markov chain) The underlying Markov chain $\{X_i\}_{i=1}^n$ is stationary with unique invariant measure π and admits a absolute spectral gap $1 - \lambda$.

Assumption 2: (Bounded Covariates) There exists an envelop function $M : X \rightarrow \mathbb{R}$ such that for any function f , $\max |f(X)| \leq M(X)$ for π -almost every X .

Assumption 3: (Bounded $(1 + \delta)$ -moments of errors) $\mathbb{E}(\varepsilon_i | X_i) = 0$. For some $\delta > 0$ and $v_\delta > 0$, $\mathbb{E}[|\varepsilon_i|^{1+\delta} | X_i] < v_\delta$.

The absolute spectral gap $1 - \lambda$ in Assumption 1 usually involves in spectral radius and geometrical ergodicity. Given the transition kernel P of a Markov chain, denote its spectral radius by $\lambda_\infty(P) = \lim_{k \rightarrow \infty} \|P^k - \pi(\cdot)\|_\pi^{1/k}$. It is known that $\lambda_\infty(P) \leq \lambda(P)$ [30], where the equality holds for reversible

Markov chain. The condition $1 - \lambda(P) > 0$ implies geometrical ergodicity. A non-zero spectral gap is closely related to other convergence criterion of Markov chains [33]. Assumption 2 requires that the covariates are bounded by an envelop function, which can be a function of time, space or any forms of random variable. The boundedness assumption is quite common in statistics and learning theory analysis [34], [35]. Assumption 3 requires errors to be with finite conditional $(1 + \delta)$ -moments, which covers a broad range of heavy-tailed noises including the student-t, the Pareto, log Normal and log Gamma et al. Now we are ready to present the main results for HMS estimator.

The following Lemmas play an important role to prove our main theoretical results, where Lemma 1 is the Bernstein inequality within Markov-dependent setting, Lemma 2 gives the localized analysis on bounding β_η and Lemma 3 presents the upper bound on the ℓ_2 error between an estimation β from a d -dimensional hypersphere and β^* .

Lemma 1: [36] Let $\{X_i\}_{i \geq 1}$ be a stationary Markov chain with invariant distribution π and right L_2 -spectral gap $1 - \lambda \in (0, 1]$. Let $f_i : \mathcal{X} \rightarrow [-c, c]$ be a bounded function with $\pi(f_i) = 0$ and $\sigma^2 = \sum_{i=1}^n \pi(f_i^2)/n$. Then, for any $0 \leq t \leq (1 - \lambda)/5c$,

Algorithm 1 Huber Regression with Markov Subsampling

- 1: **Input:** Dataset $\mathcal{D} = (\mathbf{x}_i, y_i)_{i=1}^n$, subset $\mathcal{D}_S = \emptyset$, robustification parameter τ , burn-in period: t_0 , subsample size $n_{sub} \ll n$.
- 2: Train a pilot estimator β_0 by $\beta_0 = (\mathbf{X}_r^\top \mathbf{X}_r)^{-1} \mathbf{X}_r^\top \mathbf{y}_r$, where $(\mathbf{X}_r, \mathbf{y}_r)$ are the random subsamples with size $n_0 = n_{sub}$.
- 3: Randomly select a sample \mathbf{z}_1 from \mathcal{D} , and set $\mathcal{D}_S = \mathbf{z}_1$.
- 4: **for** $2 \leq T \leq (n_{sub} + t_0)$ **do**
- 5: **while** $|\mathcal{D}_S| < T$ **do**
- 6: Randomly draw a candidate $\mathbf{z}^* = (\mathbf{x}^*, y^*)$
- 7: Calculate the acceptance probability by

$$p = \min \left\{ 1, \frac{\ell_\tau(y_T - \langle \mathbf{x}_T, \beta_0 \rangle)}{\ell_\tau(y^* - \langle \mathbf{x}^*, \beta_0 \rangle)} \right\} \quad (8)$$
- 8: Set $\mathcal{D}_S = \mathcal{D}_S \cup \mathbf{z}^*$ with probability p
- 9: If \mathbf{z}^* is accepted, set $\mathbf{z}_{t+1} = \mathbf{z}^*$
- 10: **end while**
- 11: **end for**
- 12: Denote the last n_{sub} samples as $\mathcal{D}_S = (\mathbf{X}_S, \mathbf{y}_S) = \{(\mathbf{x}_i, y_i)\}_{i=1}^{n_{sub}}$.
- 13: Solve β_τ by Huber regression (6) based on \mathcal{D}_S .
- 14: **Output:** β_τ .

we have for any $\epsilon > 0$,

$$\mathbb{P}\left(\frac{1}{n} \sum_{i=1}^n f(X_i) \geq \epsilon\right) \leq \exp\left(-\frac{n\epsilon^2}{2(A_1\sigma^2 + A_2c\epsilon)}\right), \quad (9)$$

where $A_1 = \frac{1+\lambda}{1-\lambda}$, $A_2 = \frac{1}{3}\mathbf{1}_{\lambda=0} + \frac{5}{1-\lambda}\mathbf{1}_{\lambda>0}$.

Lemma 2: [37] Suppose L is a convex function. Let $D_L(\beta_1, \beta_2) = L(\beta_1) - L(\beta_2) - \langle \nabla L(\beta_2), \beta_1 - \beta_2 \rangle$ and $\bar{D}_L(\beta_1, \beta_2) = D_L(\beta_1, \beta_2) + D_L(\beta_2, \beta_1)$. For $\beta_\eta = \beta^* + \eta(\beta - \beta^*)$ with $\eta \in (0, 1]$,

$$\bar{D}_L(\beta_\eta, \beta^*) \leq \eta \bar{D}_L(\beta, \beta^*). \quad (10)$$

Lemma 3: [12] Suppose $v_\delta < \infty$ for some $0 < \delta \leq 1$ and $(\mathbb{E}\langle \mathbf{u}, \bar{\mathbf{x}} \rangle^4)^{1/4} \leq C\|\mathbf{u}\|_2$ for all $\mathbf{u} \in \mathbb{R}^d$ and some constant $C > 0$. Moreover, let $\tau, r > 0$ satisfy $\tau \geq 2 \max\{(4v_\delta)^{1/(1+\delta)}, 4C^2r\}$ and $n \geq (\tau/r)^2(d+t)$. Then with probability at least $1 - e^{-t}$,

$$\langle \nabla L_\tau(\beta) - \nabla L_\tau(\beta^*), \beta - \beta^* \rangle \geq \frac{1}{4} \|\Sigma^{1/2}(\beta - \beta^*)\|_2^2 \quad (11)$$

uniformly over

$$\beta \in \mathbf{B}_0(r) = \{\beta \in \mathbb{R}^d : \|\Sigma^{1/2}(\beta - \beta^*)\|_2 \leq r\}.$$

Proposition 1 provides a concentration inequality for $\|\Sigma^{-1/2} \nabla L_\tau(\beta^*)\|_2$, which is fundamental to our theoretical analysis.

Proposition 1: Suppose the Markov chain samples generated by Algorithm 1 are with invariant distribution π and satisfy Assumptions 1 - 3, then for any $0 < \delta \leq 1$,

$$\begin{aligned} \|\Sigma^{-1/2} \nabla L_\tau(\beta^*)\|_2 &\leq \frac{4\sqrt{\pi}C_0A_2(d+t)\tau}{n_{sub}} \\ &+ 4C_0\sqrt{\frac{A_1v_\delta\tau^{1-\delta}(d+t)}{n_{sub}} + v_\delta\tau^{-\delta}} \end{aligned} \quad (12)$$

holds with confidence at least $1 - 2e^{-t}$, where $A_1 = \frac{1+\lambda}{1-\lambda}$, $A_2 = \frac{1}{3}\mathbf{1}(\lambda \leq 0) + \frac{5}{1-\lambda}\mathbf{1}(\lambda > 0)$.

PROOF. To bound $\|\Sigma^{-1/2} \nabla L_\tau(\beta^*)\|_2$, we first define a random vector

$$\begin{aligned} \zeta^* &= \Sigma^{-1/2} \{\nabla L_\tau(\beta^*) - \nabla \mathbb{E}L_\tau(\beta^*)\} \\ &= -\frac{1}{n_{sub}} \sum_{i=1}^{n_{sub}} \{\zeta_i \bar{\mathbf{x}}_i - \mathbb{E}(\zeta_i \bar{\mathbf{x}}_i)\}, \end{aligned} \quad (13)$$

where $\zeta_i = \varphi_\tau(\varepsilon_i)$, $\bar{\mathbf{x}}_i = \Sigma^{-1/2} \mathbf{x}_i$ with $\Sigma = \mathbb{E}(\mathbf{x}\mathbf{x}^\top)$ being positive. Assume that there exists a $1/2$ -Net $\mathcal{N}_{1/2}$ of the unit sphere \mathbb{S}^{d-1} in \mathbb{R}^d with $|\mathcal{N}_{1/2}| \leq 2^d$ such that $\|\zeta^*\|_2 \leq 2 \max_{\mathbf{u} \in \mathcal{N}_{1/2}} |\langle \mathbf{u}, \zeta^* \rangle|$. Without loss of generality, we assume \mathbf{x}_i 's are centralized. By Assumption 2, we know that \mathbf{x}_i are sub-Gaussian vectors, i.e.

$$\mathbb{P}(|\langle \mathbf{u}, \bar{\mathbf{x}} \rangle| \geq p) \leq \exp(-p^2 \|\mathbf{u}\|_2^2 / C_0^2) \quad (14)$$

for any $\mathbf{u} \in \mathbb{S}^{d-1}$ and $p \in \mathbb{R}$, where C_0 is a positive constant. We then have

$$\mathbb{E}|\langle \mathbf{u}, \bar{\mathbf{x}}_i \rangle|^k \leq C_0^k k \Gamma(k/2), \quad k \geq 1, \quad (15)$$

it immediately implies

$$\begin{aligned} \sum_{i=1}^{n_{sub}} \mathbb{E}(\zeta_i \langle \mathbf{u}, \bar{\mathbf{x}}_i \rangle)^2 &\leq 2C_0^2 \tau^{1-\delta} \sum_{i=1}^{n_{sub}} v_{i,1} = 2C_0^2 n v_\delta \tau^{1-\delta}, \\ \sum_{i=1}^{n_{sub}} \mathbb{E}(\zeta_i \langle \mathbf{u}, \bar{\mathbf{x}}_i \rangle)^k &\leq \frac{k!}{2} (C_0 \tau / 2)^{k-2} 2C_0^2 n_{sub} v_\delta \tau^{1-\delta} \end{aligned} \quad (16)$$

for $k \geq 3$. Furthermore, by Assumption 3, we have

$$\mathbb{E}[\varphi_\tau(\varepsilon)] = -\mathbb{E}[(\varepsilon - \tau)\mathbf{1}(\varepsilon > \tau)] + \mathbb{E}[(-\varepsilon - \tau)\mathbf{1}(\varepsilon < -\tau)]. \quad (17)$$

Thus for any $k > 2$,

$$|\mathbb{E}\varphi_\tau(\varepsilon)| \leq \mathbb{E}[(|\varepsilon| - \tau)\mathbf{1}(|\varepsilon| > \tau)] \leq \tau^{1-k} \mathbb{E}[|\varepsilon|^k].$$

It follows from Lemma 1 with $c = \sqrt{\pi}C_0\tau$ and $\sigma^2 = 2C_0^2v_\delta\tau^{1-\delta}$ that

$$\mathbb{P}\left\{|\langle \mathbf{u}, \zeta^* \rangle| \leq \frac{2\sqrt{\pi}C_0A_2\omega\tau}{n_{sub}} + 2C_0\sqrt{\frac{A_1v_\delta\tau^{t-1}\omega}{n_{sub}}}\right\} \geq 1 - 2e^{-\omega} \quad (18)$$

for $\forall \omega > 0$. By taking the union bound over $\mathbf{u} \in \mathcal{N}_{1/2}$, the following inequality

$$\|\zeta^*\|_2 \leq \frac{4\sqrt{\pi}C_0A_2\omega\tau}{n} + 4C_0\sqrt{\frac{A_1v_\delta\tau^{1-\delta}\omega}{n}} \quad (19)$$

holds with confidence at least $1 - 2^{d+1} \cdot e^{-\omega}$. Then we consider the deterministic part $\|\Sigma^{-1/2} \nabla \mathbb{E}L_\tau(\beta^*)\|_2$, by direct calculation

$$\|\Sigma^{-1/2} \nabla \mathbb{E}L_\tau(\beta^*)\|_2 \leq \sup_{\mathbf{u} \in \mathbb{S}^{d-1}} \frac{1}{n_{sub}} \sum_{i=1}^{n_{sub}} \mathbb{E}|\zeta_i \langle \mathbf{u}, \bar{\mathbf{x}}_i \rangle| \leq v_\delta \tau^{-\delta}.$$

Let $\omega = d + t$, by combining above inequality and (19), we obtain the stated result. \blacksquare

Theorem 1: Suppose the Markov chain samples generated by Algorithm 1 are with invariant distribution π and satisfy

Assumptions 1 - 3, then for any $t > 0$, with confidence at least $1 - 2e^{-t}$, the HMS estimator β_τ with $\tau = \frac{1}{A_\lambda} \left(\frac{n_{sub}}{d+t} \right)^{\max\{\frac{1}{1+\delta}, \frac{1}{2}\}}$ satisfies

$$\|\beta_\tau - \beta^*\|_2 \leq C_1 \lambda_{\max}(\Sigma^{1/2}) A_\lambda \left(\frac{d+t}{n_{sub}} \right)^{\min\{\frac{\delta}{1+\delta}, \frac{1}{2}\}} \quad (20)$$

provided that $n_{sub} \geq C_2(d+t)$, where $C_1, C_2 > 0$ are the constants independent of n and d , $A_\lambda = \max\left\{\sqrt{\frac{1+\lambda}{1-\lambda}}, \frac{1}{3}\mathbf{1}_{\lambda=0} + \frac{5}{1-\lambda}\mathbf{1}_{\lambda>0}\right\}$.

PROOF. To begin with, recall that $\mathbf{B}_0(r) = \{\beta \in \mathbb{R}^d : \|\Sigma^{1/2}(\beta - \beta^*)\|_2 \leq r\}$ for some $r > 0$. Define $\beta_{\tau,\eta} := \beta^* + \eta(\beta_\tau - \beta^*) \in \mathbf{B}_0(r)$, where $\eta \in (0, 1]$. Then we know from Lemma 2 that

$$\begin{aligned} & \langle \nabla L_\tau(\beta_{\tau,\eta}) - \nabla L_\tau(\beta^*), \beta_{\tau,\eta} - \beta^* \rangle \\ & \leq \eta \langle \nabla L_\tau(\beta_\tau) - \nabla L_\tau(\beta^*), \beta_\tau - \beta^* \rangle. \end{aligned} \quad (21)$$

It is easy to see $\nabla L_\tau(\beta_\tau) = 0$ due to the KKT condition. According to mean value theorem,

$$\begin{aligned} & \nabla L_\tau(\beta_{\tau,\eta}) - \nabla L_\tau(\beta^*) \\ & = \int_0^1 \nabla^2 L_\tau(t\beta_{\tau,\eta} + (1-t)\beta^*) dt (\beta_{\tau,\eta} - \beta^*) \end{aligned} \quad (22)$$

Assume there exist a constant $c > 0$ such that

$$\min_{\beta \in \mathbb{R}^d: \|\beta - \beta^*\|_2 \leq r} \lambda_{\min}(\nabla^2 L_\tau(\beta)) \geq C_0,$$

hence $C_0 \|\beta_{\tau,\eta} - \beta^*\|_2^2 \leq \|\nabla L_\tau(\beta^*)\|_2 \cdot \|\beta_{\tau,\eta} - \beta^*\|_2$, reducing the result yields

$$\|\beta_{\tau,\eta} - \beta^*\|_2 \leq C_0^{-1} \|\nabla L_\tau(\beta^*)\|_2. \quad (23)$$

Since $\beta_{\tau,\eta} \in \mathbf{B}_0(r)$, according to Lemma 3 with $r = \tau/(4C_0^2)$, we get

$$\langle \nabla L_\tau(\beta_{\tau,\eta}) - \nabla L_\tau(\beta^*), \beta - \beta^* \rangle \geq \frac{1}{4} \|\Sigma^{1/2}(\beta_{\tau,\eta} - \beta^*)\|_2^2 \quad (24)$$

with confidence at least $1 - e^{-t}$. Then by Proposition 1,

$$\begin{aligned} \|\Sigma^{-1/2} \nabla L_\tau(\beta^*)\|_2 & \leq \frac{4\sqrt{\pi} C_0 A_2 (d+t) \tau}{n_{sub}} + v_\delta \tau^{-\delta} \\ & \quad + 4C_0 \sqrt{\frac{A_1 v_\delta \tau^{1-\delta} (d+t)}{n_{sub}}} \quad (25) \\ & := r^* \end{aligned}$$

holds with confidence at least $1 - e^{-t}$. Combining (24) and (25), we know that with confidence at least $1 - 2e^{-t}$,

$$\|\beta_{\tau,\eta} - \beta^*\|_2 \leq 4r^* \quad (26)$$

provided $n \geq C_1(d+t)$, where $C_1 > 0$ is a constant depending only on C_0 . The constructed estimator $\beta_{\tau,\eta}$ lies in the interior of the ball with radius r . By the construction in the beginning of the proof, this enforce $\eta = 1$ and thus $\beta_\tau = \beta_{\tau,\eta}$. This completes the proof. \blacksquare

Remark 1: Theorem 1 indicates that the HMS estimator β_τ is consistent under moderate conditions, i.e. $\|\beta_\tau - \beta^*\| \rightarrow 0$ as $n_{sub} \rightarrow \infty$. The founding condition requires that the Markov chain generated by algorithm 1 has absolute spectral gap. HMS

almost trivially meets this condition since the corresponding Markov chain is uniformly ergodic, and hence geometrically ergodic. Moreover, the error bound of HMS only requires finite moments of error ε_i , which is weaker than sub-Gaussian error condition in linear regression models for subsampling [2], [38], [7]. We find that τ should adapt with subsample size n_{sub} , the input dimension d , the moments of error term and the dependence of underlying Markov chain. In particular, with an appropriate choice of τ , the convergence rate of HMS estimator is with $\mathcal{O}\left(\left(\frac{d}{n_{sub}}\right)^{\min\{\frac{\delta}{1+\delta}, \frac{1}{2}\}}\right)$ decay, which matches the near-optimal deviations in i.i.d. case [12]. Note that the Markov dependence impacts on τ in the way that the subsample size n_{sub} is discounted by a factor A_λ . In other words, in order to achieve τ -adaptation effect, the required subsample size increases with A_λ when transferring from i.i.d. sample setup to Markov dependence setup. Furthermore, a small value for λ implies a fast convergence rate of HMS estimator.

Theorem 2: Under the same conditions with Theorem 1, for any $t > 0$, the HMS estimator β_τ with $\tau = \sqrt{\frac{1-\lambda}{1+\lambda}} \left(\frac{n_{sub}}{(d+t) \log d} \right)^{\frac{1}{2(1+\delta)}}$ satisfies

$$\begin{aligned} & \mathbb{P}\left\{ \left\| \Sigma^{1/2}(\beta_\tau - \beta^*) - \frac{1}{n_{sub}} \sum_{i=1}^{n_{sub}} \varphi_\tau(\varepsilon_i) \bar{\mathbf{x}}_i \right\|_2 \right. \\ & \left. \geq C_3 \sqrt{\frac{1+\lambda}{1-\lambda}} \sqrt{\frac{(d+t) \log d}{n_{sub}}} \right\} \leq 3e^{-t} \end{aligned} \quad (27)$$

provided $n_{sub} \geq C_4(d+t)$, where C_3, C_4 are the constants independent n and d .

PROOF. Let $r_1 = 4r^*$, we know from the proof of Theorem 1 that

$$\mathbb{P}\{\beta_\tau \in \mathbf{B}_0(r_1)\} \geq 1 - 2e^{-t} \quad (28)$$

provided $n_{sub} \geq C_1(d+t)$. Define random process $\Phi(\beta) = L_\tau(\beta) - \mathbb{E}L_\tau(\beta)$ and

$$\Psi(\beta) = \Sigma^{-1/2} \{\nabla L_\tau(\beta) - \nabla L_\tau(\beta^*)\} - \Sigma^{1/2}(\beta - \beta^*). \quad (29)$$

Our goal is to bound $\|\Psi(\beta_\tau)\|_2 = \|\Sigma^{-1/2}(\beta_\tau - \beta^*) + \Sigma^{-1/2} \nabla L_\tau(\beta^*)\|_2$, the key step lies in bounding the supremum of empirical process $\{\Psi(\beta) : \beta \in \mathbf{B}_0(r)\}$. To achieve this goal, we need to bound $\mathbb{E}\Psi(\beta)$ and $\Psi(\beta) - \mathbb{E}\Psi(\beta)$.

Denote $\hat{\beta}$ as the convex combination of β and β^* . By mean value theorem, we see that

$$\begin{aligned} \mathbb{E}\Psi(\beta) & = \Sigma^{-1/2} \{\mathbb{E}\nabla L_\tau(\beta) - \nabla \mathbb{E}L_\tau(\beta^*)\} - \Sigma^{1/2}(\beta - \beta^*) \\ & = \{\Sigma^{-1/2} \nabla^2 \mathbb{E}L_\tau(\hat{\beta}) \Sigma^{-1/2} - \mathbf{I}_d\} \Sigma^{1/2}(\beta - \beta^*), \end{aligned} \quad (30)$$

hence

$$\sup_{\beta \in \mathbf{B}_0(r)} \|\mathbb{E}\Psi(\beta)\|_2 \leq r \times \sup_{\beta \in \mathbf{B}_0(r)} \|\Sigma^{-1/2} \nabla^2 \mathbb{E}L_\tau(\hat{\beta}) \Sigma^{-1/2} - \mathbf{I}_d\|. \quad (31)$$

We known from Assumption 2 that $\|\mathbf{x}_i\|_\infty \leq M(\mathbf{x})$, where $M(\mathbf{x}) : \mathbf{x} \rightarrow \mathbb{R}$ is a envelop function. Consider $\beta \in \mathbf{B}_0(r)$ and $\mathbf{u} \in \mathbb{S}^{d-1}$, we have

$$\begin{aligned}
 & |\mathbf{u}^\top \{\Sigma^{-1/2} \nabla^2 \mathbb{E} L_\tau(\hat{\beta}) \Sigma^{-1/2} - \mathbf{I}_d\} \mathbf{u}| \\
 &= \frac{1}{n_{sub}} \sum_{i=1}^{n_{sub}} \mathbb{E} \{ \mathbf{1}\{y_i - \langle \mathbf{x}_i, \beta \rangle \geq \tau\} \langle \mathbf{u}, \bar{\mathbf{x}}_i \rangle^2 \} \\
 &\leq \frac{1}{n_{sub}} \sum_{i=1}^{n_{sub}} \mathbb{E} \{ (\mathbf{1}\{|\varepsilon_i| \geq \tau/2\} \\
 &\quad + \mathbf{1}\{\mathbf{x}_i^\top (\beta - \beta^*) > \tau/2\}) \langle \mathbf{u}, \bar{\mathbf{x}}_i \rangle^2 \} \\
 &\leq \frac{1}{n_{sub}} \sum_{i=1}^{n_{sub}} \mathbb{E} \{ (\mathbf{1}\{|\varepsilon_i| \geq \tau/2\} + \mathbf{1}\{\|\mathbf{x}_i\|_\infty > \tau/2r\}) \langle \mathbf{u}, \bar{\mathbf{x}}_i \rangle^2 \} \\
 &\leq \frac{1}{n_{sub}} \sum_{i=1}^{n_{sub}} \mathbb{E} \{ (\mathbf{1}\{|\varepsilon_i| \geq \tau/2\} + \mathbf{1}\{M(\mathbf{x}) > \tau/2r\}) \langle \mathbf{u}, \bar{\mathbf{x}}_i \rangle^2 \} \\
 &\leq 2^{1+\delta} \sigma^2 \tau^{-1-\delta} v_\delta + \sqrt{\frac{A_1 \log d}{n_{sub}}} + 4CA_1 \sigma^4 r^2,
 \end{aligned} \tag{32}$$

which implies

$$\sup_{\beta \in \mathbf{B}_0(r)} \|\mathbb{E} \Psi(\beta)\|_2 \leq 2^{1+\delta} \sigma^2 \tau^{-1-\delta} v_\delta + \sqrt{\frac{A_1 \log d}{n_{sub}}} + 4CA_1 \sigma^4 r^2. \tag{33}$$

Next, we focus on bounding $\Psi(\beta) - \mathbb{E} \Psi(\beta)$. To this end, we first rewrite

$$\Psi(\beta) - \mathbb{E} \Psi(\beta) = \Sigma^{-1/2} \{ \nabla \Phi(\beta) - \nabla \Phi(\beta^*) \}. \tag{34}$$

Set

$$\Delta = \Sigma^{1/2} (\beta - \beta^*) \tag{35}$$

and define the empirical process

$$\bar{\Psi}(\Delta) := \Psi(\beta) - \mathbb{E} \Psi(\beta). \tag{36}$$

It is easy to check that $\bar{\Psi}(0) = 0$ and $\mathbb{E} \bar{\Psi}(\Delta) = 0$. For any $\mathbf{u}, \mathbf{v} \in \mathbb{S}^{d-1}$ and $m \in \mathbb{R}$,

$$\begin{aligned}
 & \mathbb{E} \{ m \sqrt{n} \mathbf{u}^\top \nabla_\Delta \bar{\Psi}(\Delta) \mathbf{v} \} \\
 &\leq \prod_{i=1}^{n_{sub}} \left\{ 1 + \frac{m^2}{n_{sub}} \mathbb{E} \left[\left(\langle \mathbf{u}, \bar{\mathbf{x}}_i \rangle^2 \langle \mathbf{v}, \bar{\mathbf{x}}_i \rangle^2 + \mathbb{E} |\langle \mathbf{u}, \bar{\mathbf{x}} \rangle \langle \mathbf{v}, \bar{\mathbf{x}} \rangle|^2 \right) \right. \right. \\
 &\quad \left. \left. \times e^{\frac{|m|}{\sqrt{n_{sub}}}} (|\langle \mathbf{u}, \bar{\mathbf{x}}_i \rangle \langle \mathbf{v}, \bar{\mathbf{x}}_i \rangle| + \mathbb{E} |\langle \mathbf{u}, \bar{\mathbf{x}} \rangle \langle \mathbf{v}, \bar{\mathbf{x}} \rangle|) \right] \right\} \\
 &\leq \prod_{i=1}^{n_{sub}} \left\{ 1 + e^{\frac{|m|}{\sqrt{n_{sub}}}} \frac{m^2}{n_{sub}} \mathbb{E} \left[e^{\frac{|m|}{\sqrt{n_{sub}}}} |\langle \mathbf{u}, \bar{\mathbf{x}}_i \rangle \langle \mathbf{v}, \bar{\mathbf{x}}_i \rangle| \right] \right. \\
 &\quad \left. + e^{\frac{|m|}{\sqrt{n_{sub}}}} \frac{m^2}{n_{sub}} \mathbb{E} \left[\langle \mathbf{u}, \bar{\mathbf{x}}_i \rangle^2 \langle \mathbf{v}, \bar{\mathbf{x}}_i \rangle^2 e^{\frac{|m|}{\sqrt{n_{sub}}}} |\langle \mathbf{u}, \bar{\mathbf{x}}_i \rangle \langle \mathbf{v}, \bar{\mathbf{x}}_i \rangle| \right] \right\}
 \end{aligned}$$

$$\begin{aligned}
 &\leq \prod_{i=1}^n \left\{ 1 + e^{\frac{|m|}{\sqrt{n_{sub}}}} \frac{m^2}{n_{sub}} \max_{\mathbf{w} \in \mathbb{S}^{d-1}} \mathbb{E} \left[e^{\frac{|m|}{\sqrt{n_{sub}}}} \langle \mathbf{w}, \bar{\mathbf{x}} \rangle^2 \right] \right. \\
 &\quad \left. + e^{\frac{|m|}{\sqrt{n_{sub}}}} \frac{m^2}{n_{sub}} \max_{\mathbf{w} \in \mathbb{S}^{d-1}} \mathbb{E} \left[\langle \mathbf{w}, \bar{\mathbf{x}} \rangle^4 e^{\frac{|m|}{\sqrt{n_{sub}}}} \langle \mathbf{w}, \bar{\mathbf{x}} \rangle^2 \right] \right\} \\
 &\leq \exp \left\{ m^2 e^{\frac{|m|}{\sqrt{n_{sub}}}} \left(\max_{\mathbf{w} \in \mathbb{S}^{d-1}} \mathbb{E} \left[e^{\frac{|m|}{\sqrt{n_{sub}}}} \langle \mathbf{w}, \bar{\mathbf{x}} \rangle^2 \right] \right. \right. \\
 &\quad \left. \left. + \max_{\mathbf{w} \in \mathbb{S}^{d-1}} \mathbb{E} \left[\langle \mathbf{w}, \bar{\mathbf{x}} \rangle^4 e^{\frac{|m|}{\sqrt{n_{sub}}}} \langle \mathbf{w}, \bar{\mathbf{x}} \rangle^2 \right] \right) \right\}.
 \end{aligned} \tag{37}$$

Recall that each \mathbf{x}_i is sub-Gaussian random variable, hence there exist constants A_3, A_4 depend only on C_0 such that for any $|m| \leq \sqrt{n_{sub}/A_3}$,

$$\sup_{\mathbf{u}, \mathbf{v} \in \mathbb{S}^{d-1}} \mathbb{E} \{ m \sqrt{n_{sub}} \mathbf{u}^\top \nabla_\Delta \bar{\Psi}(\Delta) \mathbf{v} \} \leq \exp \{ A_4 m^2 / 2 \}. \tag{38}$$

By Theorem A.3 in [39], we see that

$$\mathbb{P} \left\{ \sup_{\beta \in \mathbf{B}_0(r)} \|\Psi(\beta) - \mathbb{E} \Psi(\beta)\|_2 \leq 6A_4 r \sqrt{8d + 2t} \right\} \geq 1 - e^{-t} \tag{39}$$

when $n_{sub} \geq A_4(8d + 2t)$. Combing (33) and (39) together, we get

$$\begin{aligned}
 &\sup_{\beta \in \mathbf{B}_0(r_1)} \|\Sigma^{-1/2} \{ \nabla L_\tau(\beta) - \nabla L_\tau(\beta^*) \} - \Sigma^{1/2} (\beta - \beta^*)\|_2 \\
 &\leq 2^{1+\delta} \sigma^2 \tau^{-1-\delta} v_\delta + \sqrt{\frac{A_1 \log d}{n_{sub}}} \\
 &\quad + 4CA_1 \sigma^4 r_1^2 \tau^{-2} + 6A_4 \sqrt{\frac{8d + 2t}{n_{sub}}} r_1.
 \end{aligned} \tag{40}$$

with confidence at least $1 - e^{-t}$. This together with (28) yield the final result. \blacksquare

Remark 2: Theorem 2 provides a non-asymptotic Bahadur representation [18] for HMS estimator β_τ when the error terms have finite $(1+\delta)$ -th moments. It further implies that the approximation of $\beta_\tau - \beta^*$ has a sub-exponential tail. For the truncated random variable $\varphi_\tau(\varepsilon)$, we can see that

$$\begin{aligned}
 |\mathbb{E} \varphi_\tau(\varepsilon)| &= -\mathbb{E}[(\varepsilon - \tau) \mathbf{1}(\varepsilon > \tau)] + \mathbb{E}[(-\varepsilon - \tau) \mathbf{1}(\varepsilon < -\tau)] \\
 &\leq \mathbb{E}[|\varepsilon| \mathbf{1}(|\varepsilon| > \tau)] \\
 &\leq \tau^{1-\delta} \mathbb{E}[|\varepsilon|^\delta].
 \end{aligned} \tag{41}$$

This together with (27) show that the HMS estimator β_τ achieves non-asymptotic robustness against to heavy-tailed noise. Specifically, by taking

$$t = \log(n_{sub}), \tau \asymp \sqrt{\frac{1-\lambda}{1+\lambda}} \sqrt{\frac{n_{sub}}{d + \log(n_{sub})}},$$

we have

$$\begin{aligned}
 &\left\| \beta_\tau - \beta^* - \frac{1}{n_{sub}} \sum_{i=1}^{n_{sub}} \varphi_\tau(\varepsilon_i) \Sigma^{-1} \mathbf{x}_i \right\|_2 \\
 &= O \left(\sqrt{\frac{1+\lambda}{1-\lambda}} \sqrt{\frac{d + \log(n_{sub})}{n_{sub}}} \right).
 \end{aligned} \tag{42}$$

with confidence at least $1 - \mathcal{O}(n_{sub}^{-1})$. From an asymptotic viewpoint, it implies that if $d = o(n_{sub})$ as $n_{sub} \rightarrow \infty$, then for any deterministic vector $\mathbf{u} \in \mathbb{R}^d$, $\langle \mathbf{u}, \boldsymbol{\beta}_\tau - \boldsymbol{\beta}^* \rangle$ converges to $n_{sub}^{-1} \sum_{i=1}^{n_{sub}} \varphi_\tau(\varepsilon_i) \boldsymbol{\Sigma}^{-1} \mathbf{x}_i$ in distribution.

TABLE I: Statistics of real-world datasets

Datasets	# Sample size	# Features
Appliances Energy Prediction	19735	29
Poker Hand	25010	11
Gas Turbine CO and NOx Emission	36733	11
Wave Energy Converters	288000	32
PPPTS	45730	9
Beijing Multi-Site Air-Quality	382168	14

V. EXPERIMENTAL RESULTS

This section aims to evaluate the empirical performance of the proposed HMS procedure. All numerical studies are implemented with Python 3.8 under Ubuntu 16.04 operation system with 2.2 GHz CPUs and 256 GB memory.

A. Sampling Pattern

We first investigate the performance of HMS through comparing the sampling pattern to leverage sampling, gradient-based sampling (GS) and influence-based sampling (IS). A toy data is generated by $y = 2x + \varepsilon$ with $n = 50, d = 1$, where noise term comes from the student's t distribution with 2 degrees of freedom, i.e. $\varepsilon \sim t(2)$. Considering that both GS and IS require a pilot to determine the sampling probability, here we fix the pilot (marked by green dashed line) for a fair comparison. The pilot is specified by uniform sampling $n_0 = 10$ points. The turning parameter τ of HMS is set to 0.1. We plot $n_{sub} = 10$ data points (marked in red) selected by different sampling approaches, where the size denotes the corresponding assigned sampling probability. The estimators of four sampling approaches are then calculated based on the subsampled data. As illustrated in Figure 3, we see that the selected data points of HMS are more close to the oracle (marked by red real line) than competitors, hence the subsampled estimator (marked by blue dashed line) can better recover the ground-truth estimator. Moreover, it can be observed that HMS can return a reliable estimator even the pilot is deviated from the oracle, which implies its great potential on selecting informative data from the noisy data.

B. Phase Transition

Theorem (1) implies that

$$-\log(\|\boldsymbol{\beta}_\tau - \boldsymbol{\beta}^*\|) \asymp \frac{\delta}{1+\delta} \log(n_{sub}) - \frac{\delta}{1+\delta} \log(A_\lambda v_\delta),$$

$$0 < \delta \leq 1.$$

In order to validate the phase transition behavior of HMS estimator, we generate the data by (4) with $n = 10K, d = 50$ and sample independent noise from $t(df)$, which has finite $(1 + \delta)$ -th moments provided $\delta < df - 1$ and infinite df -th moment. The oracle $\boldsymbol{\beta}^*$ is generated from discrete uniform distribution $\{\pm 3, \pm 2, \pm 1, 0\}$. Following the setting in [12], we

set $n_{sub} = 1000, \delta = df - 1 - 0.05$. The turning parameter τ is specified by $\tau = \sigma \sqrt{n_{sub}/t}$, where $\sigma^2 = \frac{1}{n} \sum_{i=1}^n (y_i - \bar{y})^2$ with $\bar{y} = \frac{1}{n} \sum_{i=1}^n y_i$. The quality of the fit is measured by the absolute mean error (AME):

$$\text{AME} = \frac{1}{K} \sum_{k=1}^K \|\boldsymbol{\beta}_{\tau k} - \boldsymbol{\beta}^*\|. \quad (43)$$

Figure 4 displays the AME comparisons for HMS, least square with uniform sampling and Huber regression with uniform sampling. One can observe that the AME of HMS estimator is decreasing with the increase of δ . In particular, HMS can achieve lower AME than Huber and LS with the varying degrees of freedom. This further exhibits the significant advantages of HMS in robust regression.

C. Simulation Studies

We generate the data by $\mathbf{y} = \mathbf{X}\boldsymbol{\beta}^* + \varepsilon$ [7], where the $n \times d$ design matrix \mathbf{X} is constructed by a mixture of Gaussian $\frac{1}{2}\mathcal{N}(\mu_1, \sigma_1^2) + \frac{1}{2}\mathcal{N}(\mu_2, \sigma_2^2)$ in two different ways: (M1) $\mu_1 = -2, \sigma_1 = 3, \mu_2 = 2, \sigma_2 = 10$; (M2) $\mu_1 = 0, \sigma_1 = 3, \mu_2 = 0, \sigma_2 = 10$. We generate two different types of i.i.d noise, including log-normal distribution $\varepsilon_i \sim \text{Lognormal}(0, 1)$ and Student-t distribution $\varepsilon_i \sim t(2)$, both of them are heavy tailed and produce outliers with large variance. We denote the models combining these design matrices and noise distributions as follows: $M1(\mathbf{LN}), M1(t), M2(\mathbf{LN}), M2(t)$.

We compare the proposed HMS with several representative methods, including uniform sampling (UNIF), leverage subsampling (LEV) [3], unweighted leverage subsampling (LEVUNW), shrinkage leverage subsampling (SLEV) [5], gradient-based sampling (GS) [7] and influence-based sampling (IS) [8]. The sampling probability of SLEV is a convex combination of leverage and uniform distribution, i.e. $\pi_i^{\text{SLEV}} = \alpha \pi_i^{\text{LEV}} + (1 - \alpha) \pi_i^{\text{UNIF}}$. Here, we consider 3 different shrinkage factors $\alpha = 0.1, 0.5, 0.9$ for SLEV, denoted by SLEV0.1, SLEV0.5 and SLEV0.9 respectively. LEVUNW performs the same sampling procedure as LEV, but solves the unweighted least squares problem instead. For influence-based sampling, the sampling weight for (\mathbf{x}_i, y_i) is proportional to $\|\psi_\beta(\mathbf{x}_i, y_i)\|$, where $\psi_\beta(\mathbf{x}_i, y_i) = (y_i - \mathbf{x}_i \boldsymbol{\beta}) \sum_n^{-1} \mathbf{x}_i$ is the influence function. For GS, IS and HMS, the pilot is calculated by uniform sampling with size $n_0 = n_{sub}$, the parameter τ in HMS is specified through a grid search strategy.

For each model, we set $n = 100K, 1M$ and corresponding $d = 50, 500$. Denote sr by the sampling ratio, we set subsample size by $n_{sub} = sr * n$ with $sr = 0.001, 0.005, 0.01$. Each result is reported over $K = 100$ runs repeatedly and the mean error is calculated.

The AME comparisons for different sampling procedures are demonstrated in Figures 5 - 9, and the corresponding running time comparison is shown in Table II. Several observations can be made about the reported results. (I) Leverage based sampling procedures perform slightly worse than uniform sampling when data are corrupted by heavy tailed noises, this is because leverage can not exactly reflect the true importance of each sample in such cases. (II) GS and IS behave similar in different settings. The reason is that the design matrix \mathbf{X}

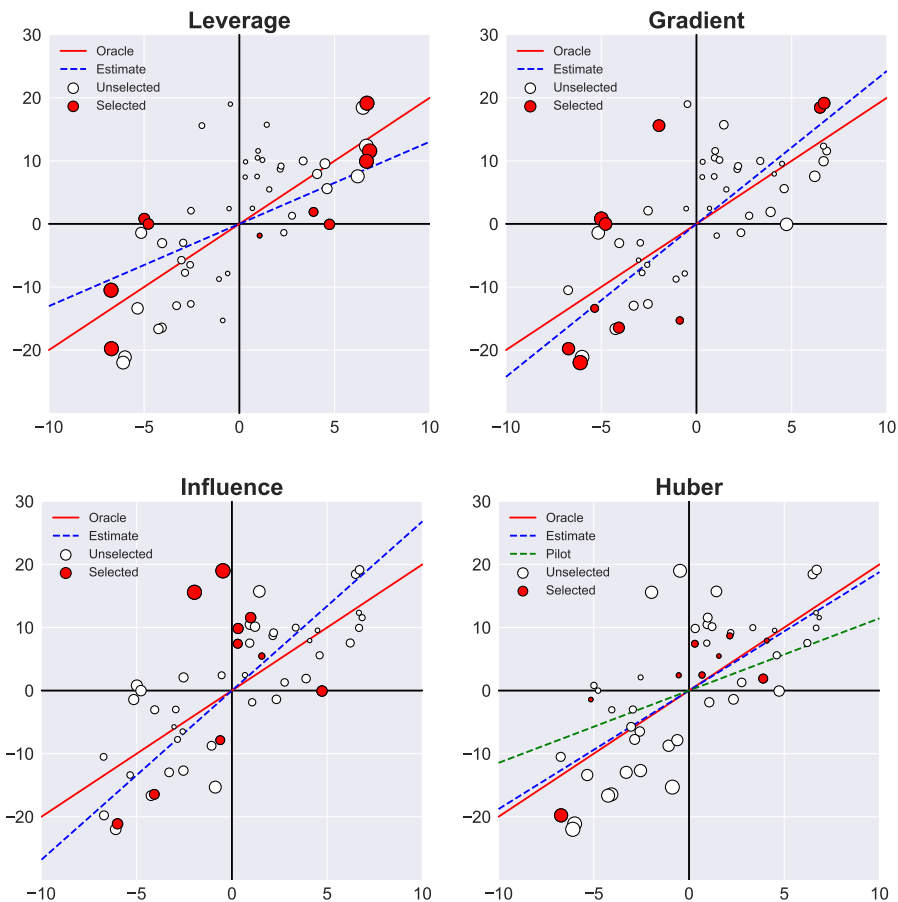


Fig. 3: Comparisons on different sampling patterns. The oracle, pilot and subsampled estimator are denoted by the red real line, the green dashed line and the blue dashed line respectively.

Methods	$n = 100K, d = 50$			$n = 500K, d = 250$			$n = 1M, d = 500$		
	$sr = 0.1\%$	$sr = 0.5\%$	$sr = 1\%$	$sr = 0.1\%$	$sr = 0.5\%$	$sr = 1\%$	$sr = 0.1\%$	$sr = 0.5\%$	$sr = 1\%$
LEV	55.9	56.1	57.6	1515.1	1597.5	1624.7	12345.4	12068.4	12947.8
SLEV	54.1	56.8	62.9	1543.8	1610.9	1640.5	9932.8	9106.2	9545.5
LEVUNW	53.8	55.6	61.1	1550.0	1580.1	1625.4	8235.8	8984.8	8918.5
GS	33.7	34.0	37.6	818.2	804.2	879.2	3505.3	3473.6	3526.8
IS	64.8	63.5	79.1	1618.5	1645.9	1794.8	8852.1	9243.0	10051.1
HMS	5.9 + 23.2	6.6 + 34.5	7.5 + 44.4	141.1 + 229.2	167.1 + 302.5	189.0 + 389.2	557.9 + 780.8	662.4 + 910.0	754.9 + 1076.4

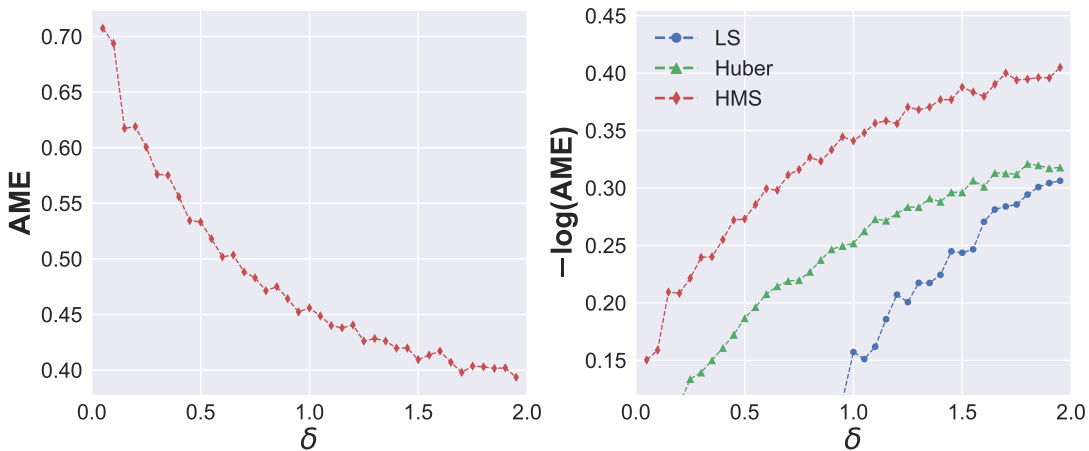
TABLE II: Comparisons on time cost (milliseconds) for different sampling methods. The time cost of HMS consists of two parts: selection of τ (left) + sampling (right).

consists of a mixture of i.i.d. Gaussian entries, leading to the covariance matrix Σ_n approximates a diagonal matrix, which makes influence function assigns similar sampling probability as gradient does. (III) GS and IS perform worse than leverage based approaches and uniform sampling when sampling ratio is small. The main reason is that both of them need a pilot to guide sampling, inefficient training for the pilot will deteriorate their performance. However, HMS performs significantly better than GS and IS with the same pilot. This demonstrates the tolerance of HMS to imperfect pilots. (IV) HMS performs much better than the other competitors in almost all settings, both in AME and running time. The efficiency improvement of HMS is still prominent even considering the time for hyperparameter (τ) selection, which implies the great advantage of HMS on selecting the informative samples under high level

noise settings.

D. Real Data Examples

We further evaluate the proposed HMS on 6 real-world datasets. Including *Appliances Energy Prediction*, *Poker Hand*, *Gas Turbine CO and NOx Emission*, *Wave Energy Converters*, *Physicochemical Properties of Protein Tertiary Structure (PPPTS)* and *Beijing Multi-Site Air-Quality*. All these datasets come from UCI machine learning repository <https://archive.ics.uci.edu/ml/datasets.php>, covering various prediction tasks. For *Poker Hand* dataset, we only use the training set. For *Wave Energy Converters* dataset, we remove 16 columns due to collinearity. For *Beijing Multi-Site Air-Quality* dataset, we remove 4 text-valued columns, and take *PM2.5* as the prediction

Fig. 4: Left: AME of HMS. Right: Comparisons on $-\log(\text{AME})$ of different sampling procedures.

Methods	Appliances Energy Prediction			Poker Hand			Gas Turbine CO and NOx Emission		
	$sr = 0.2\%$	$sr = 0.5\%$	$sr = 1\%$	$sr = 0.1\%$	$sr = 0.5\%$	$sr = 1\%$	$sr = 0.1\%$	$sr = 0.5\%$	$sr = 1\%$
UNIF	37.375(757.056)	17.544(150.132)	14.091(10.515)	20.628(39.454)	16.494(3.870)	16.145(1.733)	1.515(2.641)	1.212(0.268)	1.187(0.116)
LEV	977.049(1113.369)	30.047(832.387)	14.793(34.945)	21.687(86.551)	16.464(4.402)	16.121(1.558)	1.401(1.556)	1.198(0.147)	1.182(0.074)
SLEV1	43.437(1145.047)	32.101(786.459)	17.922(145.850)	20.199(33.124)	16.462(3.625)	16.143(1.602)	1.477(2.216)	1.204(0.170)	1.187(0.127)
SLEV5	716.760(1126.215)	39.196(1336.134)	17.582(199.610)	21.613(52.904)	16.501(3.955)	16.118(1.350)	1.428(2.594)	1.198(0.155)	1.181(0.072)
SLEV9	759.980(1476.744)	19.909(286.266)	18.714(242.235)	20.688(41.378)	16.435(2.933)	16.163(1.864)	1.386(1.148)	1.198(0.129)	1.182(0.095)
LEVUNW	23.865(118.949)	15.038(9.115)	13.849(3.739)	20.002(33.140)	16.448(3.846)	16.172(1.984)	1.355 (0.935)	1.209(0.182)	1.192(0.083)
GS	959.747(1093.527)	20.077(239.837)	21.219(754.344)	22.568(66.602)	16.425(3.497)	16.057(1.138)	1.523(3.019)	1.195 (0.145)	1.180(0.082)
IS	773.265(1675.704)	79.019(3602.502)	57.206(2274.425)	22.089(55.309)	16.391(2.900)	16.044(0.968)	1.513(2.485)	1.203(0.175)	1.180(0.069)
HMS	21.906 (106.737)	14.267 (15.968)	13.549 (6.247)	18.594 (15.623)	16.217 (1.871)	16.022 (1.044)	1.365(1.164)	1.197(0.161)	1.178 (0.052)

TABLE III: APE comparisons (mean \pm standard deviation) for different sampling methods for real datasets

Methods	Wave Energy Converters			Physicochemical Properties of Protein Tertiary Structure			Beijing Multi-Site Air-Quality Data		
	$sr = 0.1\%$	$sr = 0.5\%$	$sr = 1\%$	$sr = 0.1\%$	$sr = 0.5\%$	$sr = 1\%$	$sr = 0.1\%$	$sr = 0.5\%$	$sr = 1\%$
UNIF	55.611(9.120)	52.892(1.638)	52.594(0.680)	22.946(33.494)	19.074(8.027)	18.647(4.511)	27.930(9.177)	27.207(1.000)	27.125(0.330)
LEV	55.553(9.456)	52.875(1.724)	52.585(0.783)	20.328(11.959)	18.494(2.109)	18.298(0.891)	27.535(2.552)	27.162(0.455)	27.109(0.205)
SLEV1	55.305(8.762)	52.866(1.634)	52.585(0.665)	22.336(49.774)	18.509(3.508)	18.299(0.915)	27.698(4.926)	27.176(0.541)	27.118(0.350)
SLEV5	55.528(8.142)	52.853(1.439)	52.591(0.826)	20.207(13.829)	18.399(1.568)	18.269(0.842)	27.586(2.942)	27.156(0.467)	27.108(0.301)
SLEV9	55.425(9.317)	52.885(1.679)	52.579(0.795)	20.024(12.033)	18.446(1.916)	18.295(0.834)	27.523(2.037)	27.158(0.457)	27.106(0.208)
LEVUNW	55.365(6.857)	52.906(1.462)	52.625(0.786)	19.562(6.400)	18.700(1.997)	18.558(1.131)	27.832(6.767)	27.338(1.295)	27.259(0.736)
GS	55.905(10.413)	52.753 (1.170)	52.504 (0.528)	21.165(16.045)	18.463(1.907)	18.265(0.872)	27.346(1.187)	27.100(0.157)	27.076 (0.066)
IS	55.738(9.943)	52.756(1.259)	52.517(0.581)	21.364(20.183)	18.474(1.561)	18.427(2.645)	27.343(1.236)	27.104(0.172)	27.078(0.082)
HMS	54.982 (6.715)	52.789(1.323)	52.560(0.683)	19.472 (15.802)	18.299 (1.580)	18.089 (0.871)	27.185 (0.479)	27.085 (0.075)	27.089(0.063)

TABLE IV: APE comparisons (mean \pm standard deviation) for different sampling methods for real datasets

target. The results are averaged over $K = 100$ runs of each experiment, and the average prediction errors (APE):

$$\text{APE} = \frac{1}{K} \sum_{k=1}^K \|\hat{\mathbf{y}}_k - \mathbf{y}\|$$

are reported in Table III and IV. It can be observed that HMS can achieve superior performance in these regression tasks. Specifically, HMS almost always reach the lowest error and standard deviation when sampling ratio remains small, this shows the great potential of applying HMS to deal with big data. For the Gas Emission, Wave Energy and Air-Quality datasets, HMS sometimes yields sub-optimal results comparing to other methods. This is because that in real-world scenarios, the properties of the noise are unknown, and some of the assumptions are not guaranteed to be hold, i.e. bounded covariates or bounded $1 + \delta$ order error moments. The convergence of HMS is thus influenced and results in sub-optimal samples. However, HMS still achieves the highest performance in most conditions, which demonstrates its outstanding robustness over other methods.

VI. DISCUSSION AND FUTURE RESEARCH

In this paper, we propose a Markov subsampling strategy based on Huber criterion (HMS) to achieve robust estimation. The deviation bounds of HMS estimator are established. We find that the HMS estimator exhibits a similar phase transition to that in the independent setup. The only difference is up to a factor $\sqrt{\frac{1-\lambda}{1+\lambda}}$, defined by the absolute spectral gap λ of underlying Markov chain. Extensive studies on large scale simulations and real data examples demonstrate the effectiveness of HMS. There are many opportunities along the line of current research, such as how to deduce the lower bounds for HMS estimator and how to perform HMS in high dimensional case. All these problems deserve further research.

REFERENCES

- [1] Y. Zhang, J. Duchi, and M. Wainwright, "Divide and conquer kernel ridge regression: A distributed algorithm with minimax optimal rates," *J. Mach. Learn. Res.*, vol. 16, no. 1, pp. 3299–3340, 2015.
- [2] P. S. Dhillon, Y. Lu, D. Foster, and L. Ungar, "New subsampling algorithms for fast least squares regression," in *Proc. 26th Int. Conf. Neural Inf. Proc. Syst.*, 2013, pp. 360–368.

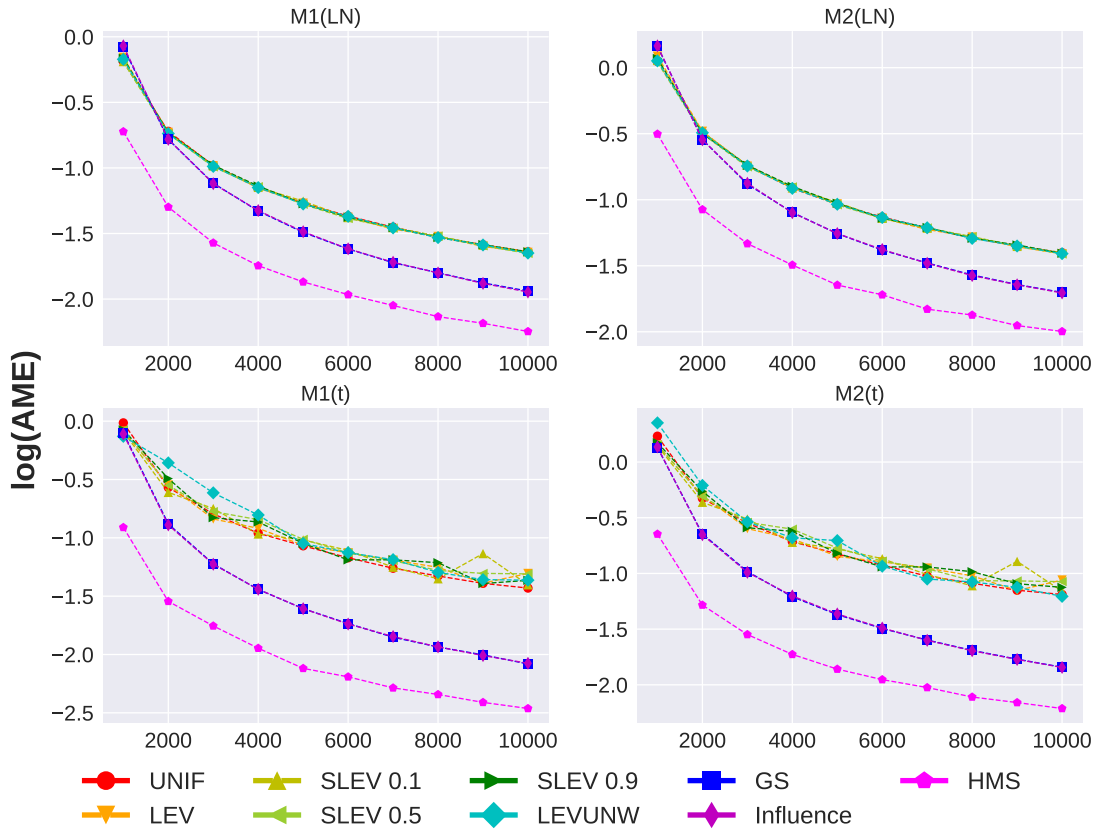


Fig. 5: Comparisons on AME of different sampling procedures. In all settings, we vary the subsample size $n_{sub} = sr * n$ with $sr = [0.002, 0.004, 0.006, 0.008, 0.01]$.

- [3] P. Drineas, M. Magdon-Ismael, M. W. Mahoney, and D. P. Woodruff, "Fast approximation of matrix coherence and statistical leverage," *J. Mach. Learn. Res.*, vol. 13, no. Dec, pp. 3475–3506, 2012.
- [4] P. Drineas, M. W. Mahoney, S. Muthukrishnan, and T. Sarlós, "Faster least squares approximation," *Numerische Mathematik*, vol. 117, no. 2, pp. 219–249, 2011.
- [5] P. Ma, M. W. Mahoney, and B. Yu, "A statistical perspective on algorithmic leveraging," *J. Mach. Learn. Res.*, vol. 16, no. 1, pp. 861–911, 2015.
- [6] A. Rudi, D. Calandriello, L. Carratino, and L. Rosasco, "On fast leverage score sampling and optimal learning," in *Proc. 32nd Int. Conf. Neural Inf. Proc. Syst.*, 2018, pp. 5677–5687.
- [7] R. Zhu, "Gradient-based sampling: An adaptive importance sampling for least-squares," in *Proc. 30th Int. Conf. Neural Inf. Proc. Syst.* Citeseer, 2016, pp. 406–414.
- [8] D. Ting and E. Brochu, "Optimal subsampling with influence functions," in *Proc. 32nd Int. Conf. Neural Inf. Proc. Syst.*, 2018, pp. 3654–3663.
- [9] P. J. Huber, "Robust estimation of a location parameter," in *Breakthroughs Statist.* Springer, 1992, pp. 492–518.
- [10] S. Lambert-Lacroix, L. Zwald *et al.*, "Robust regression through the huber's criterion and adaptive lasso penalty," *Electron. J. Statist.*, vol. 5, pp. 1015–1053, 2011.
- [11] L. Wang, C. Zheng, W. Zhou, and W.-X. Zhou, "A new principle for tuning-free huber regression," *Statist. Sinica*, 2020.
- [12] Q. Sun, W. Zhou, and J. Fan, "Adaptive huber regression," *J. Amer. Statist. Assoc.*, vol. 115, no. 5293, pp. 254–265, 2020.
- [13] J. Fan, Y. Guo, and B. Jiang, "Adaptive huber regression on markov-dependent data," *Stochastic Processes and their Applications*, 2019.
- [14] B. Chen, W. Zhai, and Z. Huang, "Low-rank elastic-net regularized multivariate huber regression model," *Applied Mathematical Modelling*, vol. 87, pp. 571–583, 2020. [Online]. Available: <https://www.sciencedirect.com/science/article/pii/S0307904X20302389>
- [15] G. P. Meyer, "An alternative probabilistic interpretation of the huber loss," in *Proceedings of the IEEE/CVF Conference on Computer Vision and Pattern Recognition (CVPR)*, June 2021, pp. 5261–5269.
- [16] Y. Wang, X. Zhong, F. He, H. Chen, and D. Tao, "Huber additive models for non-stationary time series analysis," in *International Conference on Learning Representations*, 2022. [Online]. Available: <https://openreview.net/forum?id=9kpuB2bgnim>
- [17] R. R. Bahadur, "A note on quantiles in large samples," *Ann. Math. Statist.*, vol. 37, no. 3, pp. 577–580, 1966.
- [18] X. He, Q.-M. Shao *et al.*, "A general bahadur representation of m-estimators and its application to linear regression with nonstochastic designs," *Ann. Statist.*, vol. 24, no. 6, pp. 2608–2630, 1996.
- [19] R. Vershynin, *High-dimensional probability: An introduction with applications in data science*. Cambridge University Press, 2018, vol. 47.
- [20] D. Rudolf, "Explicit error bounds for markov chain monte carlo," *arXiv:1108.3201*, 2011.
- [21] O. Catoni, "Challenging the empirical mean and empirical variance: a deviation study," in *Annales l'IHP Probabilités Statistiques*, vol. 48, no. 4, 2012, pp. 1148–1185.
- [22] P. W. Holland and R. E. Welsch, "Robust regression using iteratively reweighted least-squares," *Commun. Statist. Theory Methods*, vol. 6, no. 9, pp. 813–827, 1977.
- [23] J. Yu, H. Wang, M. Ai, and H. Zhang, "Optimal distributed subsampling for maximum quasi-likelihood estimators with massive data," *J. Amer. Statist. Assoc.*, vol. 0, no. 0, pp. 1–29, 2020.
- [24] H. Wang, "More efficient estimation for logistic regression with optimal subsamples," *J. Mach. Learn. Res.*, vol. 20, no. 132, pp. 1–59, 2019.
- [25] P. J. Rousseeuw and A. M. Leroy, *Robust regression and outlier detection*. John Wiley & sons, 2005, vol. 589.
- [26] P.-L. Loh *et al.*, "Statistical consistency and asymptotic normality for high-dimensional robust m -estimators," *Ann. Statist.*, vol. 45, no. 2, pp. 866–896, 2017.
- [27] T. Gong, B. Zou, and Z. Xu, "Learning with ℓ_1 -regularizer based on markov resampling," *IEEE Trans. Cybernetics*, vol. 46, no. 5, pp. 1189–1201, 2015.
- [28] J. V. Burke, F. E. Curtis, A. S. Lewis, M. L. Overton, and L. E. Simões, "Gradient sampling methods for nonsmooth optimization," *Numer. Nonsmooth Optim.*, pp. 201–225, 2020.

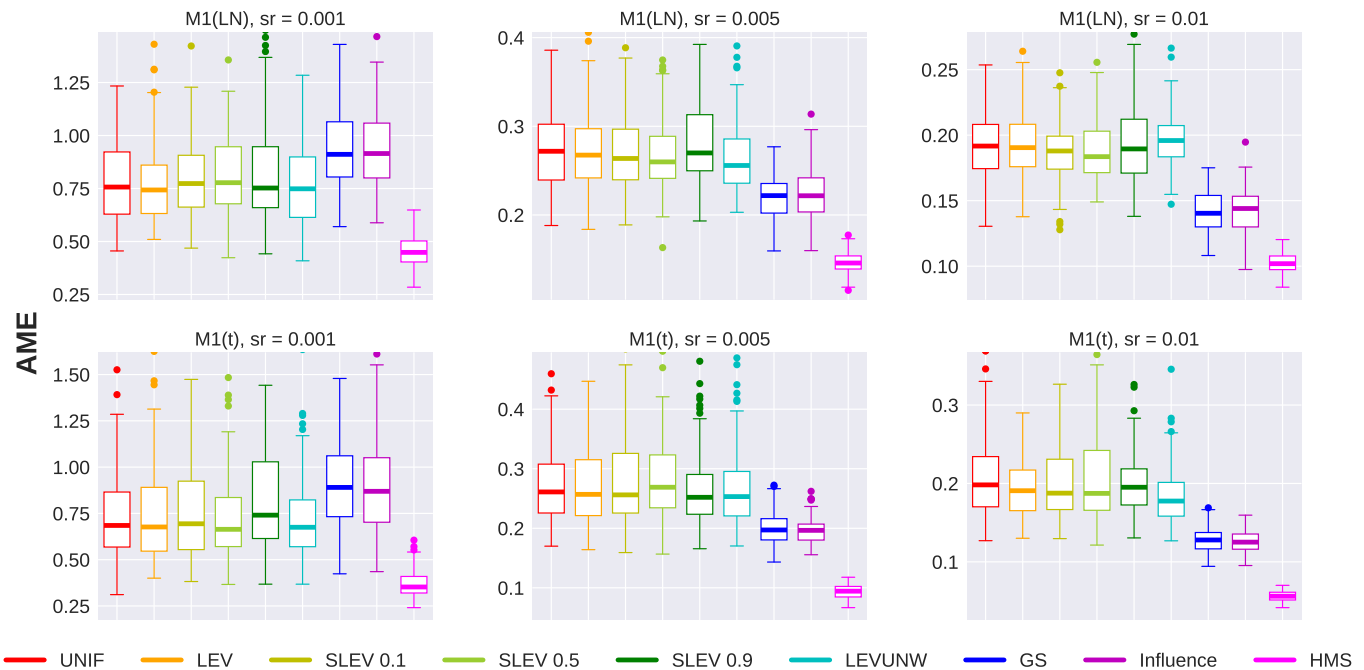


Fig. 6: Boxplots of AME for different subsampling methods ($n = 10K, d = 50$)

- [29] T. Sun, Y. Sun, and W. Yin, “On markov chain gradient descent,” in *Proc. 32nd Int. Conf. Neural Inf. Proc. Syst.*, 2018, pp. 9918–9927.
- [30] S. P. Meyn and R. L. Tweedie, *Markov chains and stochastic stability*. Springer Science & Business Media, 2012.
- [31] D. Down, S. P. Meyn, and R. L. Tweedie, “Exponential and uniform ergodicity of markov processes,” *Ann. Prob.*, vol. 23, no. 4, pp. 1671–1691, 1995.
- [32] J. L. Morales and J. Nocedal, “Remark on “algorithm 778: L-bfgs-b: Fortran subroutines for large-scale bound constrained optimization”,” *ACM Trans. Math. Softw.*, vol. 38, no. 1, pp. 1–4, 2011.
- [33] G. Roberts, J. Rosenthal *et al.*, “Geometric ergodicity and hybrid markov chains,” *Electron. Commun. Probab.*, vol. 2, pp. 13–25, 1997.
- [34] J. Fan, B. Jiang, and Q. Sun, “Hoeffding’s lemma for markov chains and its applications to statistical learning,” *arXiv:1802.00211*, 2018.
- [35] F. Cucker and D. X. Zhou, *Learning theory: an approximation theory viewpoint*. Cambridge University Press, 2007, vol. 24.
- [36] B. Jiang, Q. Sun, and J. Fan, “Bernstein’s inequality for general markov chains,” *arXiv:1801.00341*, 2018.
- [37] J. Fan, H. Liu, Q. Sun, and T. Zhang, “I-lamm for sparse learning: Simultaneous control of algorithmic complexity and statistical error,” *Ann. Statist.*, vol. 46, no. 2, p. 814, 2018.
- [38] B. McWilliams, G. Krumpalmer, M. Lucic, and J. M. Buhmann, “Fast and robust least squares estimation in corrupted linear models,” in *Proc. 27th Int. Conf. Neural Inf. Proc. Syst.*, 2014, pp. 415–423.
- [39] V. Spokoiny, “Bernstein-von mises theorem for growing parameter dimension,” *arXiv:1302.3430*, 2013.

APPENDIX

In this section, we add supplementary experiments on different data scales. In Figure 10, 11 and 12, we give additional experiment results of sampling patterns with different subsampling strategies. We keep the same settings as “A. Sampling Pattern” and set number of samples $n = \{50, 200\}$, distribution of noises $\varepsilon \sim \{\mathbf{t}(2), \mathbf{Lognormal}(0, 1)\}$. In all of these settings, we can derive the same conclusion that HMS achieves the lowest estimation error, even the pilot is deviated from the oracle.

In Figure 13 and 14, we give additional experiment results of the phase transition behavior. Again, we keep the same parameter settings as “B. Phase Transition” and alter the simulation data size to $n = 5000, d = 25, n_{sub} = 50$ and $n = 20000, d = 100, n_{sub} = 200$. As can be seen, HMS still achieves lower AME than Huber and LS consistently under various data scales.

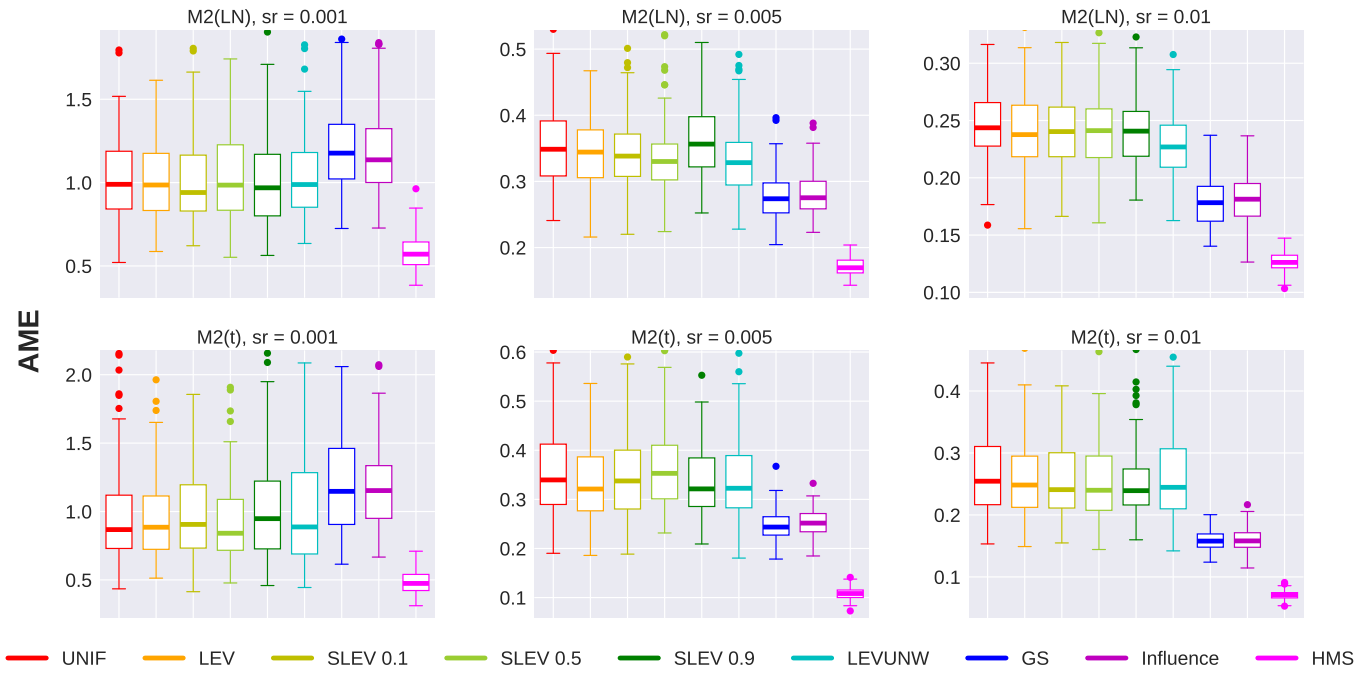


Fig. 7: Boxplots of AME for different subsampling methods ($n = 10K, d = 50$)

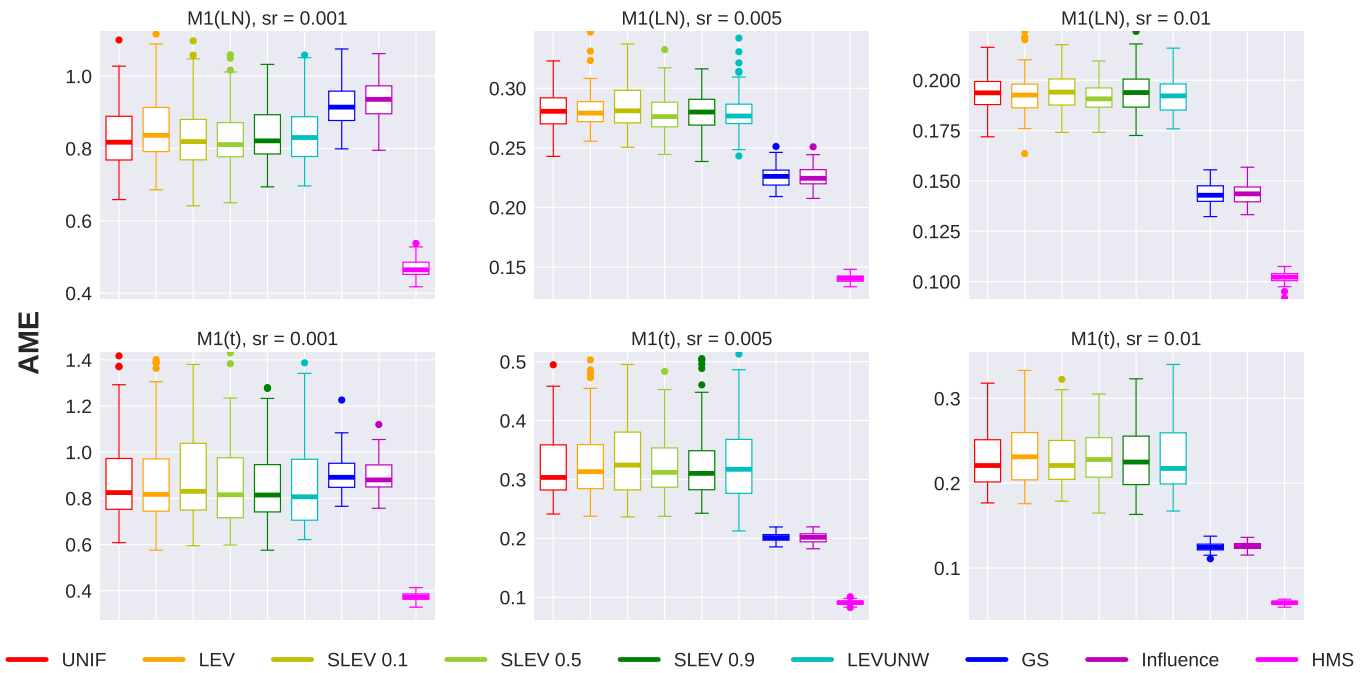


Fig. 8: Boxplots of AME for different subsampling methods ($n = 1M, d = 500$)

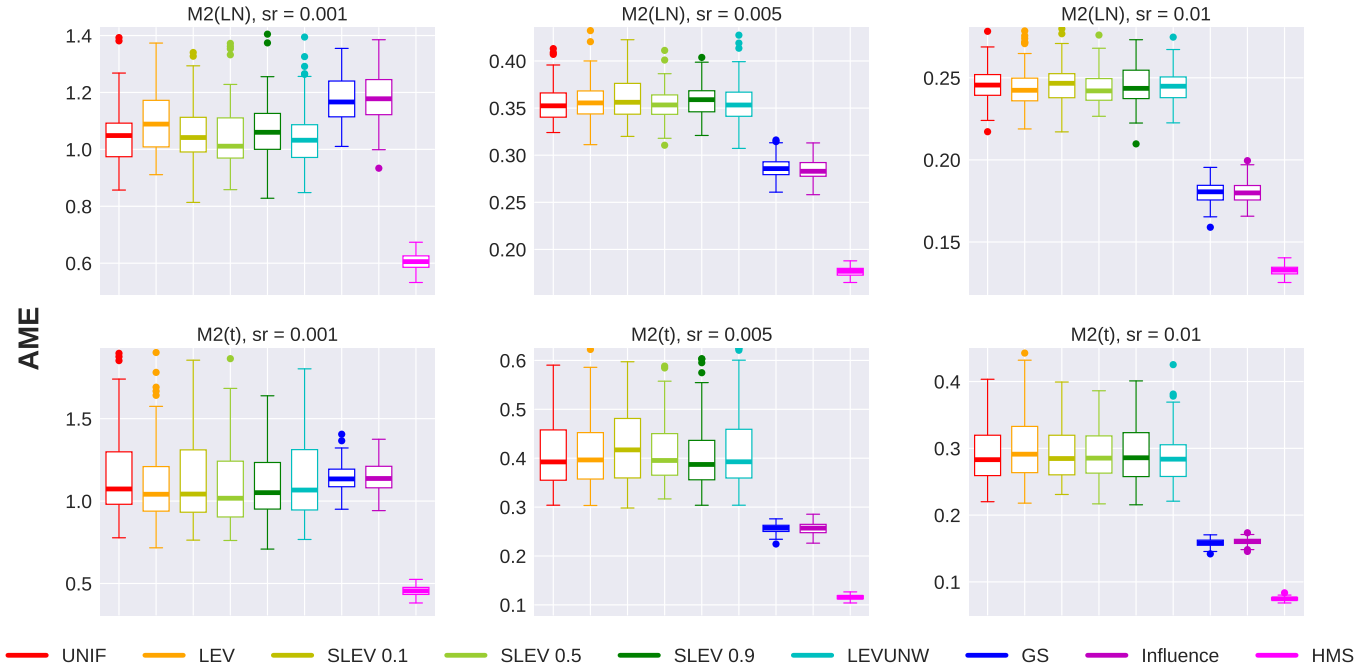


Fig. 9: Boxplots of AME for different subsampling methods ($n = 1M, d = 500$)

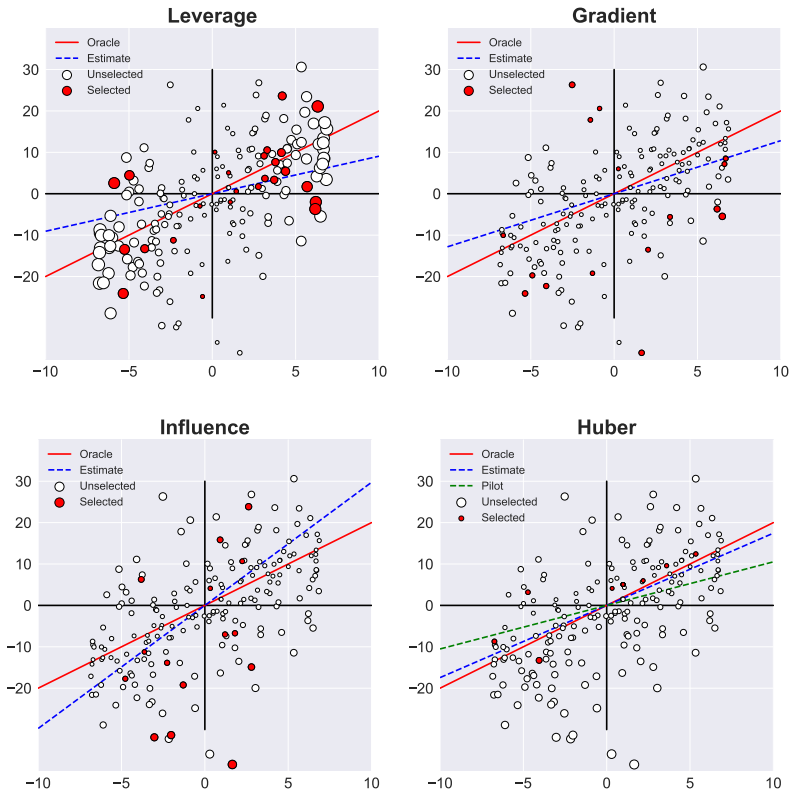


Fig. 10: Comparisons on different sampling patterns with $n = 200$ and $\varepsilon \sim \mathbf{t}(2)$.

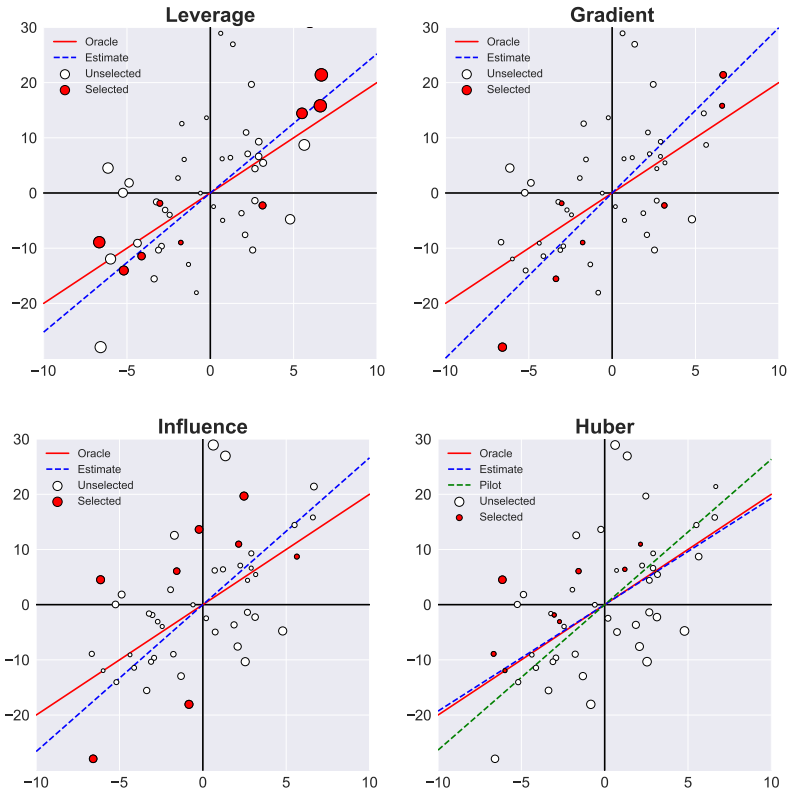


Fig. 11: Comparisons on different sampling patterns with $n = 50$ and $\varepsilon \sim \text{Lognormal}(0, 1)$.

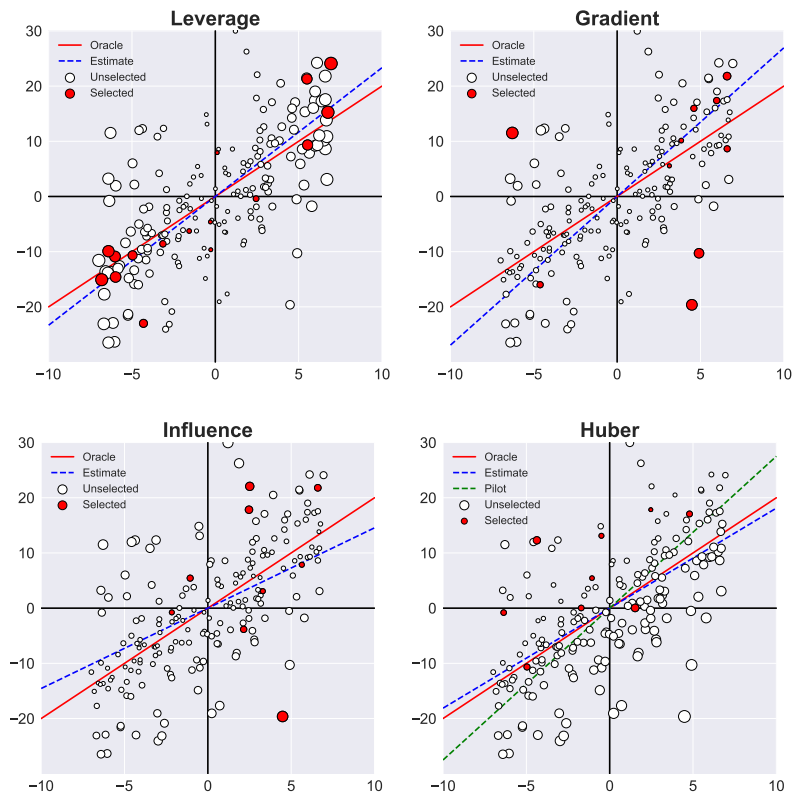


Fig. 12: Comparisons on different sampling patterns with $n = 200$ and $\varepsilon \sim \text{Lognormal}(0, 1)$.

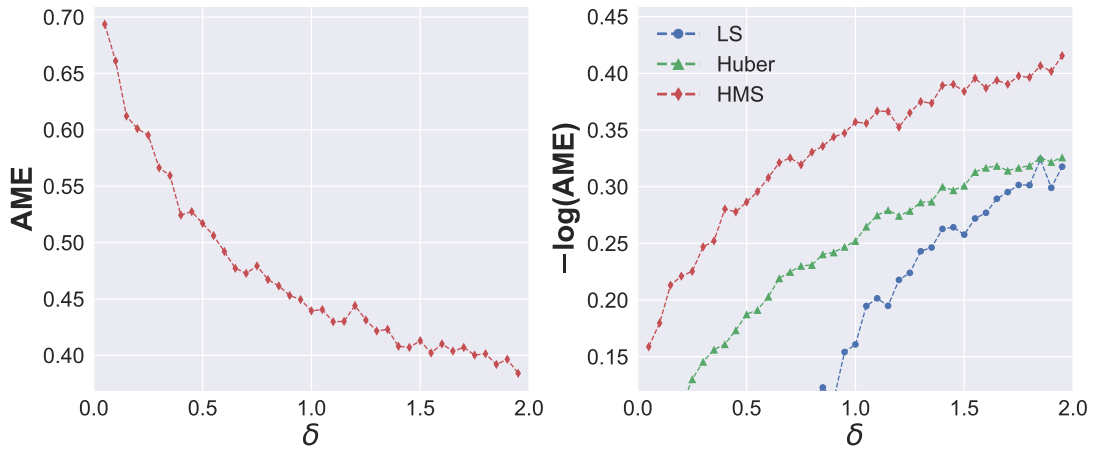


Fig. 13: Comparisons on AME of different sampling procedures with $n = 5000$, $d = 25$ and $n_{sub} = 50$.

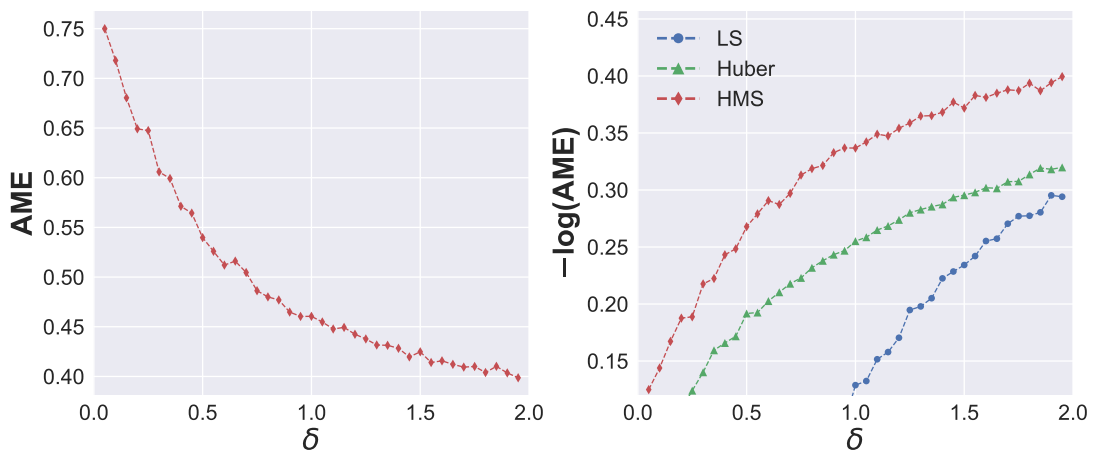


Fig. 14: Comparisons on AME of different sampling procedures $n = 20000$, $d = 100$ and $n_{sub} = 200$.